From DEPARMENT OF BIOSCIENCES AND NUTRITION
Karolinska Institutet, Stockholm, Sweden

ACTIVATION OF RETROVIRUS SPIKES FOR MEMBRANE FUSION

Robin Löving

Stockholm 2011

Published by Karolinska Institutet. Printed by US-AB.

ISBN 978-91-7457-362-6

To my family

ABSTRACT

Retroviruses are enveloped viruses that use reverse transcriptase to convert their RNA genome into DNA which is integrated into the host DNA. They enter into the cell by a membrane fusion process. In this the viral membrane fuses with that of the cell so that the internal capsid of the virus with the genome can be released into the cell cytoplasm. The fusion is mediated by the spike protein in the viral membrane. In my thesis work I have studied how the spike proteins of two retroviruses, the human immunodeficiency virus typ 1 (HIV-1) and a murine leukemia virus (MLV), are able to catalyze the fusion reaction. I found that defined changes in the spike structure mediated different steps in the fusion process. As the spikes constitute the major target for neutralizing antibodies against the virus the structures of the spikes and its natural intermediate forms should facilitate development of retroviral vaccines and drugs, which are so heavily needed in the case of HIV-1.

The spike is made as a trimeric transmembrane protein in the infected cell and incorporated into virus by budding at the cell surface. The spike then guides the virus to an uninfected cell for virus entry by membrane fusion. These tasks put several demands on the spike function. A key event is its binding to a receptor molecule of the target cell. This triggers, or activates the spike for membrane fusion. However, the activation should not occur in the cell where the virus is produced. Therefore, premature activation is prevented by synthesis of the spike in a precursor form, unable to fuse. Proteolytic cleavage of the spike, before receptor binding, then creates a mature form of the spike, which can be activated by the receptor. I have studied the maturation process of the Moloney (Mo)-MLV spike.

The Mo-MLV spike precursor matures by two proteolytic cleavages. The first one is by the furin enzyme of the producer cell and this forms the receptor binding peripheral subunit (SU) and the fusion active transmembrane subunit (TM) of the spike. The second cleavage is made by the viral protease and occurs in newly released virus. It separates a short peptide, called the R-peptide, from the membrane internal cytoplasmic tail (CT) of TM. I have studied the R-peptide cleavage using biochemical techniques and found that the cleavages in the trimeric spike occur by positive cooperativity, i.e. the cleavage of one subunit facilitates the cleavages of the two other TM subunits in the spike. This helps the spike to reach full fusion activity soon after virus budding. The activation of the spike by the receptor involves dissociation of SU from TM so that the latter can fuse the viral and the cell membranes. I also found that the R-peptide interfered with this dissociation step by inhibiting isomerization of the intersubunit disulfide in the Mo-MLV spike, which normally occurs soon after receptor binding.

Using HIV-1 I studied how the primary receptor CD4 activated the spike for binding to the coreceptor, a chemokinreceptor. In this case I used cryo-electron microscopy and image processing to determine the 3D structures of the native unliganded and the CD4 bound spike. The spikes were released from virus, with or without bound CD4, by solubilization with TX-100 and isolated for EM analysis by density gradient centrifugation. I found that the native spike had an open cage-like structure, where the protomeric unit formed a common roof and a lobe, and a leg on the side. This structure was verified by the unique fitting of the earlier determined atomic structure of the core portion of the peripheral subunit. CD4 binding caused the roof part to lift up probably to enable coreceptor binding and to open the roof for the fusion activated TM.

List of publications

This thesis is based on the following papers, which are referred to in the text by their Roman numbers I-IV.

I. Michael Wallin, **Robin Löving**, Maria Ekström, Kejun Li, and Henrik Garoff. (2005). Kinetic Analyses of the Surface-Transmembrane Disulfide Bond Isomerization-Controlled Fusion Activation Pathway in Moloney Murine Leukemia Virus. *Journal of Virology. 79(22), 13856-64.*

II. **Robin Löving**, Kejun Li, Michael Wallin, Mathilda Sjöberg and Henrik Garoff. (2008). R-Peptide Cleavage Potentiates Fusion-Controlling Isomerization of the Intersubunit Disulfide in Moloney Murine Leukemia Virus Env. *Journal of Virology. 82(5). 2594-7.*

III. **Robin Löving**, Malin Kronqvist, Mathilda Sjöberg and Henrik Garoff. (2011). Cooperative Cleavage of the R-Peptide in the Env Trimer of the Moloney Murine Leukemia Virus Facilitates its Maturation for Fusion Competence. *Journal of Virology. 85(7). 3262-9*

IV. Shang-Rung Wu[1], **Robin Löving**[1], Birgitta Lindqvist, Hans Hebert, Philip J.B. Koeck, Mathilda Sjöberg and Henrik Garoff. (2010). Single-Particle Cryoelectron Microscopy Analysis Reveals the HIV-1 Spike as a Tripod Structure. *PNAS. 107(44). 18844-9.*

[1.] Authors have contributed equally to this work.

TABLE OF CONTENTS

1. INTRODUCTION

Viruses are intracellular parasites using target cells for producing new virus particles able to spread and invade more cells. There are many types of viruses and they can be divided into two main groups, enveloped viruses that are surrounded by a lipid membrane and naked viruses containing an outer protein shell. My thesis covers two different retroviruses, Moloney murine leukemia virus (Mo-MLV) and Human Immunodeficiency Virus type 1 (HIV-1), belonging to the enveloped virus group. These enveloped viruses fuse, or merge, their viral lipid membrane with the cell membrane, as a first step towards infection. Through this process the viral core with the genome gains entrance into the cell cytoplasm. I have focused my investigations to how this fusion mechanism is controlled.

1.1 RETROVIRUS CLASSIFICATION AND PATHOGENESIS.

Retroviruses are divided into seven different genera (Table 1). The first three genera are classified as simple retrovirus and the four last ones are described as complex retrovirus. The simple retroviruses contain the viral genes gag, pol and env, encoding the minimal number of proteins needed for a retrovirus infection. The complex retroviruses encode several accessory proteins.

Table 1. Retrovirus genera.

Genus	***Example***
Alfaretrovirus	Avian leucosis virus (ALV)
Betaretrovirus	Mouse mammory tumour virus (MMTV)
Gammaretrovirus	Murine leukemia virus (MLV)
Deltaretrovirus	Human T-cell leukemia virus (HTLV)
Epsilonretroviruses	Walley dermal sarcoma virus
Lentivirus	Human immunodeficiency virus (HIV)
Spumaretrovirus	Human foamy virus (HFV)

MLV is a simple retrovirus and belongs to the gammaretrovirus genus. The MLV group is further divided into subgroups depending on their use of host cell receptor for entry (Table 2). Ecotropic MLV, like Mo-MLV, uses the cationic amino acid transporter MCAT-1 and can only infect mouse and rat cells (Albritton et al., 1989; Davey et al., 1997). Amphotropic MLV can infect murine as well as none murine cells (also human cells) and uses the receptor PIT-2, a sodium dependent transporter of phosphate (Miller et al., 1994; van Zeijl et al., 1994). Xenotropic MLV was first isolated from mouse but

the tropism differed from eco- and amphotropic viruses in that it could not infect mouse cells. Surprisingly it could efficiently infect cells of others species such as human, rabbit and cat. The receptor used by Xenotropic MLV is called XPR1 and is a protein of unknown function. However homologous proteins in yeast (SYG1) and plant (PHO) have been associated to signal transduction, phosphate sensing and transport (Tailor et al., 1999; Yang et al., 1999). The last subgroup of MLV is called polytropic. This group of viruses also uses the XPR1 receptor for entry. Even though xenotropic and polytropic MLV uses the same receptor they have different tropism. This has been mapped to variation in the extracellular loops of the receptor (Kozak, 2010). It is interesting to note that all receptors identified for gamma retroviruses have several transmembrane segments and are all believed to work as transporters of cargo from the outside to the inside of the cell. The transport properties of these receptors are not believed to have a function as such during entry. The receptor is thought to function only as a binding site, activating the entry mechanism of the virus (Wang et al., 1994; Soll et al., 2010).

Table 2. MLV subgroups.

Virus	***Example***
Ecotropic MLV	Moloney (Mo)-MLV and Friend (Fr)-MLV
Amphotropic MLV	4070A MLV
Polytropic MLV	Mink cell focus-inducing MLV (MCF-MLV)
Xenotropic MLV	Xenotropic murine leukemia virus-related virus (XMRV)

The pathogenesis of MLV have recently gained a lot of interest when a xenotropic murine leukemia virus-related virus (XMRV) was suggested to be associated with chronical fatigue syndrome (CFS) and prostate cancer (Urisman et al., 2006; Lombardi et al., 2009; Schlaberg et al., 2009; Lo et al., 2010). These proposals are still controversial. Many other laboratories have been unable to detect XMRV in either CFS or prostate cancer patients. These differences in results have been explained by geographic differences in the distribution of XMRV, false positive results when using sensitive PCR assays, contamination of virus particles either from mice or humans and difficulties regarding endogenous retroviruses and how this can cause false positive results in serum and cell cultures (Hohn et al., 2009; Aloia et al., 2010; Groom et al., 2010; Hue et al., 2010; Oakes et al., 2010; Robinson et al., 2010; Switzer et al., 2010). Even though XMRV in human disease is under debate it has been shown that XMRV is a human pathogen and can infect and spread in human cell lines, especially in prostate carcinoma cells (Rodriguez and Goff, 2010; Stieler et al., 2010). With the knowledge that MLV can induce leukemia and lymphoma in mice, it is also possible that XMRV can cause disease in humans. In a mouse model for XMRV infection it has been shown that the virus can infect the spleen, blood and brain i.e. a similar tissue selectivity as

previously described for ecotropic and amphotropic MLV (Chatis et al., 1983; Rosen et al., 1985; Evans and Morrey, 1987; Sakuma et al., 2011). Further research in this field will tell us if XMRV or any other MLV related viruses are the source of human disease.

The second virus in focus in my thesis is the complex retrovirus HIV-1, belonging to the lentivirus genus. Lentiviruses are divided into five serogroups reflecting the host they are associated with (see Table 3). One common aspect of lentiviruses is that the host cells are CD4 positive T cells. Most lentivirus use CD4 as a primary receptor for entry, one exception is FIV using the CD134 receptor (de Parseval et al., 2004; Shimojima et al., 2004).

Table 3. Lentivirus subgroups.

Virus	***Examples***
Bovine Lentivirus	Bovine immunodeficiency virus (BIV)
Equine Lentivirus	Equine infectious anemia virus (EIAV)
Feline Lentivirus	Feline immunodeficiency virus (FIV)
Ovine/caprine Lentivirus	Visna Virus
Primate Lentivirus	Human immunodeficiency virus type 1 (HIV-1)

To complete entry lentiviruses also need to interact with a seven transmembrane protein, a coreceptor. In most cases the coreceptor is either the chemokine receptor CCR5 or CXCR4, but other similar coreceptors have been identified (Deng et al., 1996; Feng et al., 1996; Shimizu et al., 2009). Since lentiviruses target cells of the immune system, the infection creates immune deficiency when the target cells start to die. In the case of HIV-1 infection, this stage is known as Acquired Immunodeficiency Syndrome (AIDS) and the patient has an increased risk of dying by secondary infections. It has been noted that only a few percent of the CD4 positive T-cells are actually infected and still most of the helper T-cells die. In a recent study this phenomenon was shown to be caused by abortive HIV-1 infection in nonepermissive CD4 T-cells. It was found that the nonepermissive T-cells contained partial HIV reverse transcripts. Further it was shown that the accumulation of these transcripts activated the innate antiviral response followed by cell death (Doitsh et al., 2010). In 2009, 33 million people were infected by HIV (WHO homepage) and there is a vast need for a definite prevention of the virus. Efficient HIV drugs exist today, but a downside with these is the immense costs associated with the treatment making it less available for underprivileged third world countries. Another down side of current treatments is the development of drug resistance. Consequently the drugs are only prolongers of life, not an absolute cure.

1.2 RETROVIRUS PARTICLES AND THEIR LIFECYCLE.

I will start by describing the simple retrovirus, MLV and its lifecycle. Thereafter differences compared with the complex retrovirus HIV-1 will be issued. MLV are spherical, lipid surrounded viruses with a size of about 100 nm in diameter. The viral genome consists of a diploid, single stranded positive sense RNA, and contains three main coding domains common to all retrovirus, gag, pol and env, encoding the Gag and Gag-Pol polyproteins and the Env protein. The Gag polyprotein contains the structural protein units for the capsid (CA), nucleocapsid (NC), p12 and the matrix protein (MA) providing shape and structure for the virus particle. The CA proteins create a core surrounding the viral genome, the NC protein bind to the viral RNA inside the core and the MA protein bind to the inner side of the viral membrane. Pol contains the protein units for the viral enzymes, reverse transcriptase (RT), integrase (IN) and the protease (PR) needed to complete the viral lifecycle. The Env proteins make up the glycoproteins located in the viral membrane needed for entry of the virus into the host cell. Env binds to a specific host cell receptor that triggers a fusion mechanism merging the viral membrane with the cellular membrane. The purpose is to release the viral capsid core with the genome in the cytoplasm to initiate an infection. First the viral RT converts the virus RNA into double stranded DNA. This creates a pre-integration complex (PIC) believed to consist of the retrovirus genome, RT, IN, CA and NC together with cellular proteins. Recently it was also shown that p12 is required for a functional PIC (Prizan-Ravid et al., 2010). The PIC is then transported into the cell nucleus where the viral DNA becomes inserted into the host genome by a mechanism driven by the viral IN enzyme. The integrated form of the virus is known as the provirus. From this the cellular transcription machinery replicates new viral genomes, which are also used for synthesis of viral proteins. Env synthesis is initiated on free ribosomes and then cotranslationally inserted into the endoplasmic reticulum (ER). After trimerization into spikes, Env is transported through the secretory pathway to the plasma membrane. The Gag and Gag-Pol polyproteins are synthesized on free ribosomes in the cell cytoplasm. The Gag interacts with transcribed unspliced viral RNA which will initiate Gag oligomerisation. Subsequently a myristoylated site in MA is exposed and targets the complex to the plasma membrane. Here, further Gag oligomerization forms a lattice below the membrane driving budding, spike association and release of virus particles. To complete budding retroviruses use the cellular endosomal sorting complex required for transport (ESCRT). This contains more than 20 proteins and associated factors and is required for several membrane fission events in eukaryotic cells. During or soon after budding the viral PR cleaves the Gag and Gag-Pol polyproteins into their separate proteins. In addition, for MLV, a 16 amino acid long peptide (the R-peptide) is cleaved by the viral PR at the C-terminal end of Env, i.e. in the membrane internal endo-domain also called the cytoplasmic tail (CT) (Coffin et al., 1997; Hunter, 1997; Rosenberg and Jolicoeur, 1997; Swanstrom and Wills, 1997; Vogt, 1997).

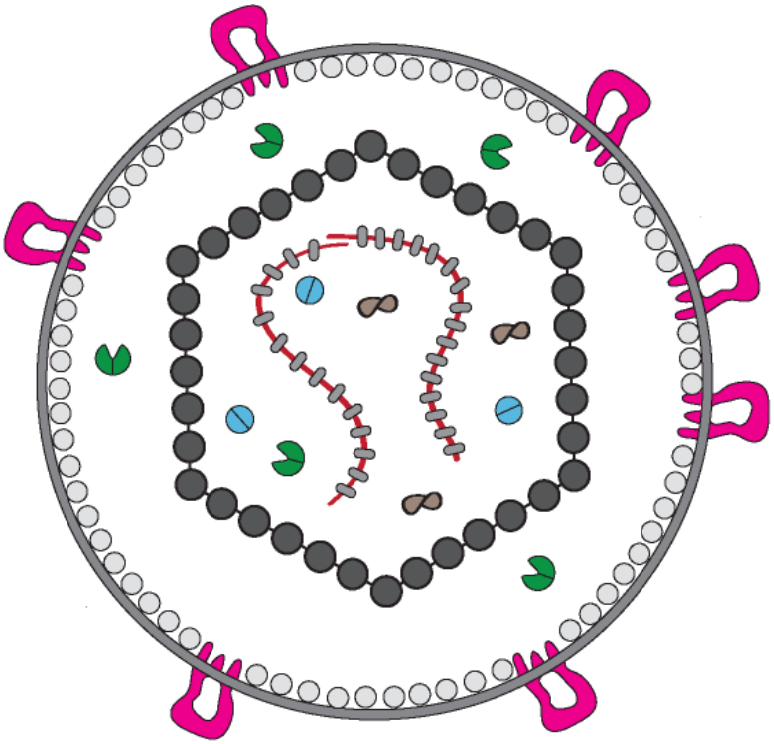

Fig1. Schematic illustration of a retrovirus particle. The virion is a spherical particle surrounded by a phospholipid bilayer which harbours the viral spike proteins (pink). On the inside of the bilayer is the MA attached (light grey circles). Several copies of the CA make up an internal core (dark grey circles). For MLV the core has icosahedral symmetry whereas HIV-1 contains a cone shaped core. The core encages two copies of the viral RNA genome (red strings) that are in complex with the NC (oval shaped beads). Included in the particle is also the viral specific enzymes; PR (green), RT (brown) and IN (blue).

Many aspects of the MLV lifecycle also apply to HIV-1. One main difference is that HIV-1 can infect both dividing and non-dividing cells. Other differences include the HIV genome that is somewhat more complex compared to MLV. The HIV Gag lacks the p12, instead it contains the protein p6 which is needed for efficient virus release from infected host cells. HIV also expresses six accessory proteins; Tat, Rev, Nef, Vpr, Vif and Vpu. Tat enhances viral transcription, Rev then transports the viral RNA from the nucleus into the cytoplasm.

The remaining accessory proteins have evolved to evade and counteract the host defense mechanisms. During recent years it has been shown that retroviral host cells contain antiviral restrictions factors targeting different stages of the retrovirus lifecycle. Three main restriction factors have been found until now; the APOBEC3G, the tetherin and the TRIM5α. The APOBEC3G protein incorporates into virus particles and induces lethal hypermutations of the retroviral genome. The tetherin protein prevents virus release by clamping budded virus particles to the plasma membrane. The TRIM5α protein binds to incoming cores during the initial stage of the infection, preventing release of the viral genome into the cell cytoplasm. It has been shown that two HIV-1 accessory proteins directly target these innate restriction factors. Vif binds to ABOBEC3G targeting it for degradation and thereby prevents it from being incorporated into viral particles. Vpu counteracts tetherin and thereby allows efficient virus release from the infected cell. Vpu has also been shown to down regulate CD4 to escape the immunsystem and avoid superinefection. Nef enhances viral replication and is also shown to down regulate the expression of several surface molecules essential for the immune system, i.e. MHC class I and CD4 at the plasma membrane. Vpr is known to arrest the cell cycle at the G2 phase. In addition Vpr has been associated with induction of cell death and is needed for efficient infection of HIV in macrophages (Bieniasz, 2009; Kirchhoff, 2010).

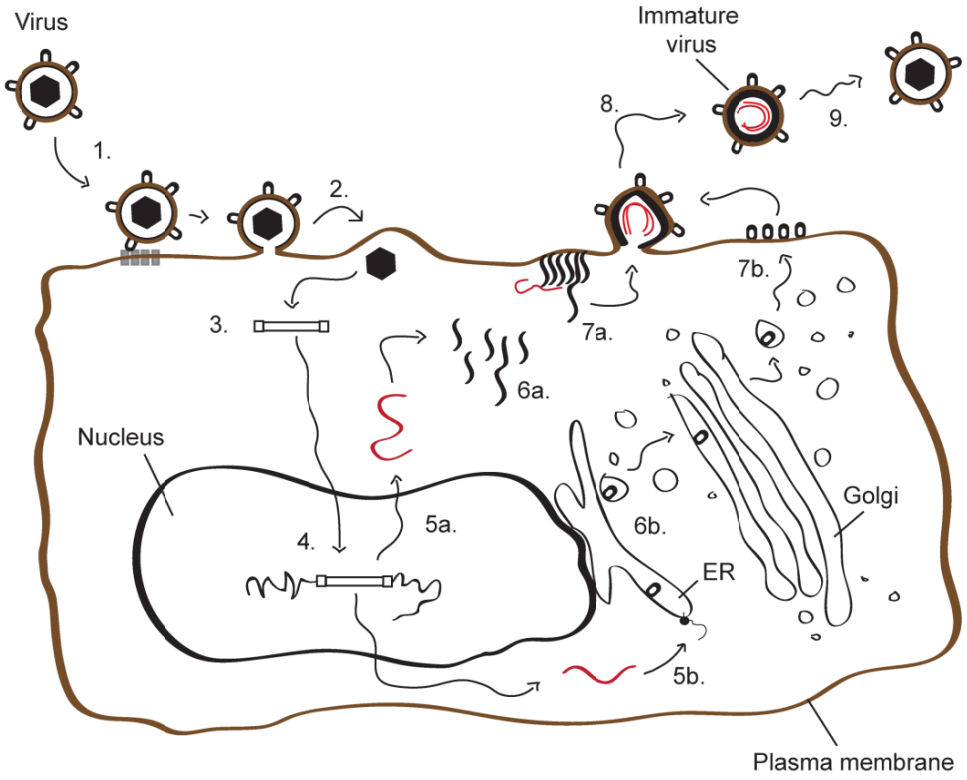

Fig 2. Schematic picture of the retrovirus lifecycle. (1) The virus particle binds to specific host cell receptors. (2) Activation of the viral spike protein to fuse the viral membrane with the cell plasmamembrane. As a result the viral core with the genome is released into the cell cytoplasm. (3) The viral RT transforms the RNA genome into double stranded DNA. (4) The viral DNA is transported into the cell nucleus were the viral IN inserts the DNA into the host cell genome. This form of the virus is known as the provirus, which uses the cellular transcription machinery to produce mRNA encoding for viral proteins. (5a) Unspliced viral mRNA is translated, on free ribosomes, in the cytoplasm to the polyproteins Gag and Gag-Pol. (6a) Gag and Gag-Pol interact with unspliced viral RNA initiating Gag oligomerization. This targets the Gag and Gag-Pol to the inside of the plasma membrane. (5b) Spliced viral RNA is used for translation of Env, which is cotranslationally inserted into the ER (6b) and further transported and modified through the secretory pathway. (7a and 7b) The Env spike is transported to the spot in the plasma membrane were Gag and Gag-Pol oligomerization cause membrane budding (8) and release of virus particles from the infected cell. (9) At first the virus particles are immature and not capable to infect a new cell. The viral PR matures the virion by cleaving the Gag and Gag-Pol into their separate proteins.

1.3 VIRUS ENTRY.

1.3.1 MEMBRANE REMODELING DURING FUSION.

Membrane fusion is the process when two separate lipid membranes merge together into one. This is a fundamental cellular process responsible for e.g. intracellular trafficking, nerve cell signaling, fertilization and tissue formation. The fusion of two lipid membranes is not a spontaneous event; it needs input energy from an external source. In cells and enveloped viruses fusion proteins have evolved. They lower the energy barrier for membrane fusion in a controlled manner. Figure 3, summarizes the paradigm of how two lipid membranes fuse together. As the lipid bilayers have a natural repulsion from each other (Fig 3A) the fusion protein first has to drag the membrane into close contact (estimated to a few nanometers). Local pulling of the membranes then creates point like protrusions that minimizes the membrane repulsion allowing the membranes to come into still closer proximity (Fig 3B). Then both outer leaflets of the lipid membranes merge together and form what is known as a hemifusion stalk (Fig 3C). The stalk structure is a key intermediate in most theoretical models and is predicted to minimize the bending energy needed for membrane fusion. It is possible to create stable hemifusion intermediates by reversing the membrane curvature at the fusion site. The classic example is addition of the lipid lysophosphatidylcholine (LPC), which has a big head group, to the outer leaflet. This cause the membrane to obtain the positive curvature that stabilizes the stalk (Fig 3F). Normal fusion is believed to continue with radial expansion of the hemifusion stalk to form a dimpling where the distal monolayers combine into a single bilayer, the hemifusion diaphragm (Fig 3D). Finally, lateral tensions in the diaphragm opens up a fusion pore that expands into full fusion (Fig 3E). (Chernomordik and Kozlov, 2003, 2008; Kozlov et al., 2010).

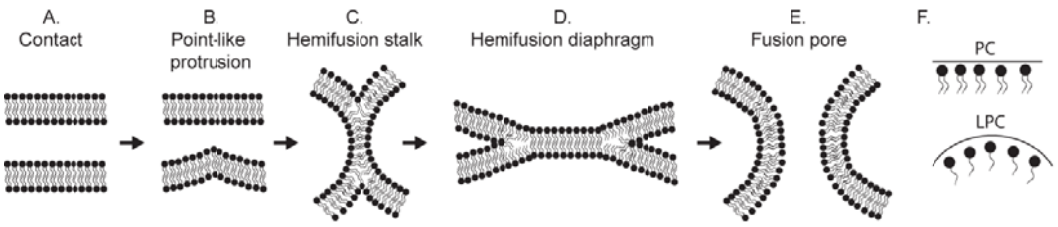

Fig 3. Fusion of two lipid bilayers. (A) Two lipid bilayers are brought into close contact. (B) A point-like membrane protrusion allows the membranes to come into still closer proximity. (C) The outer leaflets of the membranes merge and form a hemifusion stalk. (D) Expansion of the stalk forms a hemifusion diaphragm. (E) The fusion pore forms from the hemifusion diaphragm. (F) Illustration of how the shape of lipids affect the membrane curvature. Phosphatidylcholine (PC) have a cylindrical shape and forms almost flat monolayers. Lysophosphatidylcholine (LPC) has the shape of an inverted cone forming a positive (convex) membrane curvature (modified from Chernomordik et al. 2003).

1.3.2 FUSION PROTEINS

The best characterized fusion proteins are those of enveloped viruses and the cellular SNARE protein complex. The SNAREs are responsible for vesicle merging during intracellular trafficking and neurotransmitter release in nerve cells. The viral fusion proteins are membrane proteins that are used to merge the viral lipid membrane with a cell membrane, either at the plasma membrane or in intracellular vesicles, to release the viral genome into the cell. These systems are different in many aspects, but the mechanicstic outcome is the same, i.e. insertion of a fusion peptide into the target membrane followed by conformational changes within the proteins dragging the two membranes together for fusion. Below I will summarize the present knowledge about how viral fusion proteins function.

1.3.3 VIRAL FUSION PROTEINS

Enveloped viruses are surrounded by a lipid bilayer derived from the host cell during virus budding. This membrane shields the capsid with the genetic material of the virus until it is delivered into the cytoplasm of a new host cell to initiate an infection. The delivery takes place as membrane fusion event between the virus membrane and the membrane of the host cell. Virus membrane fusion can occur at the plasma membrane at neutral pH as in several retroviruses, were receptor (and possibly coreceptor) binding is the sole trigger for fusion.

Table 4.

Classification of viral fusion proteins	
• *Class I*	*Fusion active subunit (virus)*
Retrovirus	TM (MLV) and gp41 (HIV)
Orthomyxovirus	HA2 (Influenza virus)
Filovirus	GP2 (Ebola virus)
Coronavirus	S2 (SARS virus)
Paramyxovirus	F1 (Simian virus 5)
• *Class II*	
Flavivirus	E (Dengue virus)
Togavirus	E1 (Semliki forest virus)
• *Class III*	
Rhabdoviruses	G (Vesicular stomatitis virus)
Herpesvirus	gB (Herpes Simplex Virus)

Other viruses, e.g. influenza virus, have evolved to use receptor mediated endocytosis and entry then takes place in an endocytic compartment. These viruses frequently use acidic pH as a trigger for membrane fusion. Other variants of fusion triggering exist, e.g. ALV need both receptor binding and low pH and the Ebola- and SARS- viruses need proteolysis in the endosomes (Mothes et al., 2000; Chandran et al., 2005; Matsuyama et al., 2005; Simmons et al., 2005). Even though viruses use different entry strategies the function of the fusion protein is remarkable conserved.

Most viral fusion proteins are made as precursors in the RER where they also form trimers. When the protein pass through the *trans*-Golgi cellular furin cleaves the precursor into two subunits, the N-terminal, peripheral subunit and the C-terminal transmembrane subunit. The peripheral subunit carries the properties needed for receptor binding to the host cell, whereas the transmembrane subunit carries the fusion activity. The peripheral subunit also suppresses the fusion potential stored in the transmembrane subunit (Fig 4A). However, receptor binding, and sometimes low pH, dissociates the peripheral subunit from the transmembrane subunit. This activates certain conformational changes within the transmembrane subunit. First an extended "pre-hairpin" trimer structure of the transmembrane subunit is believed to be formed. This inserts a hydrophobic domain, the fusion peptide, into the target membrane (Fig 4b). Thereafter the prehairpin structure back folds upon itself, creating a "hairpin" trimer structure (post fusion structure). The back folding drags the two membranes together for membrane fusion (Fig 4C and 4D). The fusion proteins of the different viruses have been divided into different classes depending on what kind of secondary structure the transmembrane subunit is composed of. The Class 1 fusion proteins are characterized by a central α-helical coiled-coil structure in the transmembrane subunit, creating a six helical bundle upon hairpin formation. The class 2 fusion proteins are dominated by β-sheet structures in the fusion active subunit and the class 3 fusion proteins have a mixed secondary structure (Table 4). The retroviruses carry class 1 fusion proteins as does viruses such as orthomyxoviruses, paramyxoviruses, coronaviruses and filoviruses. The fusion protein of influenza virus, an orthomyxovirus, is called the hemagglutinin (HA) and is the classical example of a class 1 fusion protein. Both the native pre-fusion structure and the low pH activated post fusion structure of the HA have been solved using X-ray crystallography (Skehel and Wiley, 2000; Kielian and Rey, 2006; Harrison, 2008).

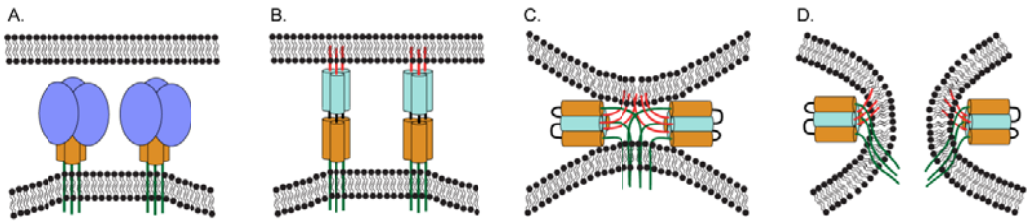

Fig 4. Activation of a class I viral fusion protein. (A) The spike in its native, prefusion state, where the peripheral subunit (blue) protects and suppresses activation of the transmembrane subunit. (B) Fusion activation, either by low pH or receptor binding, dissociates the peripheral subunit thereby allowing the metastable transmembrane subunit to refold. This results first in formation of an extended trimeric coiled coil that exposes the fusion peptide for insertion into the target membrane. Helical regions in the N-terminal ecto-domain (N-helix, cyan) and in the C-terminal ecto-domain (C-helix, brown) as well as the fusion peptide (red) are shown. (C and D) Two copies of the extended prehairpin structure are shown to backfold upon itself creating six-helical bundles. This pulls the viral and the cell membranes together for fusion (modified from Skehel, and Wiley, 2000).

1.3.4 THE MODEL FOR VIRAL FUSION PROTEINS, THE INFLUENZA HA.

The HA is a homotrimer first synthesized as a fusion inactive precursor, known as HA0. Upon passage through the Golgi complex the HA0 is proteolytically cleaved by cellular furin. This cleavage potentiates HA for fusion by creating two subunits, the C-terminal transmembrane subunit (HA2) and the N-terminal peripheral subunit (HA1). HA1 carries the receptor binding properties and HA2 contains the ability to fuse membranes.

It is believed that HA1 works like a clamp on HA2 suppressing its fusion potential. Receptor binding triggers virus internalization into cellular endosomes where the low pH activates HA for membrane fusion (Huang et al., 1981; White et al., 1981). It is known that HA2 exists as a metastable structure in the native HA. This means that HA2 has energy loaded into its conformation when clamped by HA1. When the virus particle enters into the low pH environment of the endosome, HA1 activates fusion by releasing its clamp on HA2. This in turn releases the folding energy of HA2 enabling it to undergo conformational changes. These involve formation of an extended alfa helical region that allows the fusion peptide to become exposed and inserted into the target membrane. Thereafter the HA2 chain undergoes a jack-knife-like chain reversal, which brings the viral and cellular membranes in sufficiently close contact to trigger membrane fusion. The model where the metastable HA2 is prevented from activation until an energy threshold is reached is called the spring loaded model. Normally the threshold is overcome by low pH, but can be reached also by unspecific protein destabilizing like heat treatment or incubation with urea (Carr and Kim, 1993; Skehel

and Wiley, 2000). This is similar to what have been observed for the retroviruses ALV and MLV and is believed to be a general property among the viral fusion proteins (Smith et al., 2004; Wallin et al., 2005). The conformational changes by the HA2 during fusion activation are assumed to be general for all type 1 viral fusion proteins. However, there are significant variation between different viruses how the changes in the fusion proteins are controlled and how they are triggered.

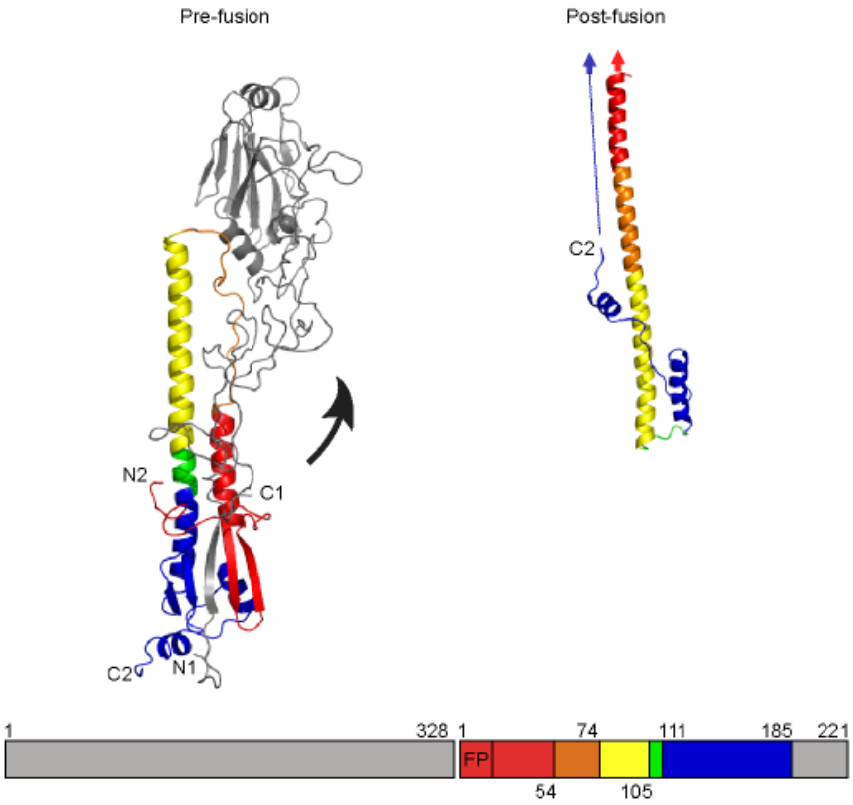

Fig. 5. Activation of the influenza virus HA2 for membrane fusion. The structure of the prefusion HA1-HA2 subunit complex is shown to the left and the postfusion structure of the HA2 subunit to the right. Below is a linear map of the HA1-HA2 with HA2 regions multicolored. Corresponding colors are used in the HA2 structures. The core of HA2 is formed by a long α-helix (yellow, green and blue) that is linked to a backfolded helix (red) by a loop (orange) at its N-terminus. The fusion peptide (red) extends the red helix and forms the N-terminus of HA2. Activation involves a loop-to-helix transition of the orange loop. This results in an N-terminal extension of the core helix and relocation of the fusion peptide to its end (red arrow). Further the transition of the green part of the central helix into a loop allows backfolding of the blue part of the core helix together with its downstream sequences. N1 and C1 indicate the N-terminal and C-terminal ends of HA1, and N2 and C2 those of HA2. The PDB ID codes for the pre- and post-fusion forms are 2HMG and IQU1.

1.4 THE RETROVIRUS SPIKE

The Env protein is the fusion protein for retroviruses and this is synthesized in the ER as an uncleaved heavily glycosylated precursor polypeptide chain; Pr80env for MLV and gp160 for HIV. After forming a homotrimer it is transported and modified in the secretory pathway. During passage through the Golgi complex Env is cleaved by furin into the peripheral surface subunit (SU for MLV, gp120 for HIV-1) carrying the receptor binding properties and the C-terminal, fusion active transmembrane subunit (TM for MLV, gp41 for HIV-1). The furin cleavage or, in case of MLV, the furin cleavage and the viral protease cleavage of the R-peptide are believed to release the Env trimers in a metastable conformation that is loaded with the energy needed to execute fusion (Hallenberger et al., 1992).

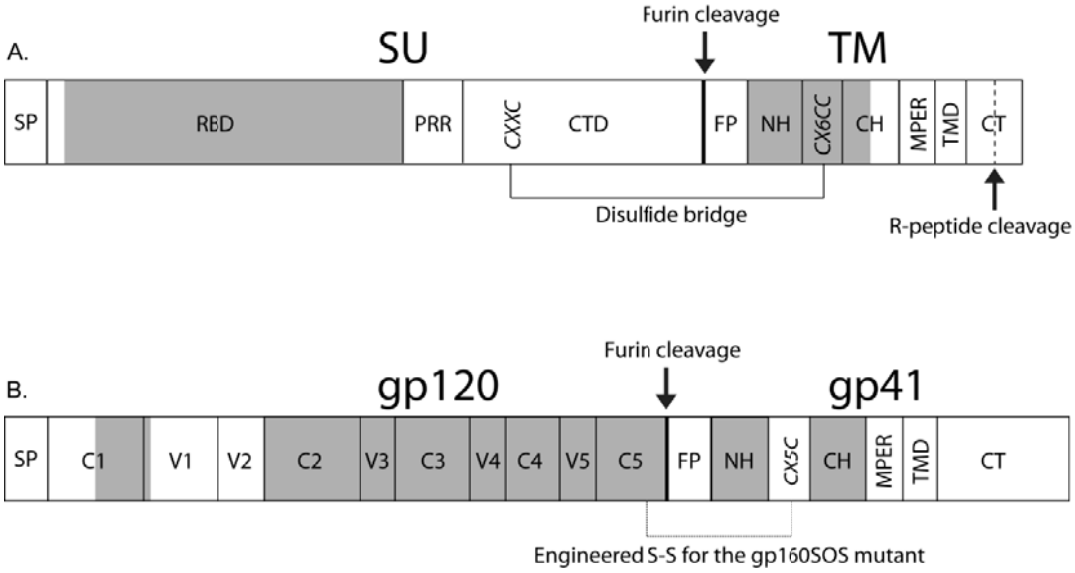

Fig 6. Domain structures of MLV Env (A) and HIV-1 gp (B). Domain abbreviations in MLV Env: SP, signal peptide; RBD, receptor binding domain; PRR, proline rich region; CTD, C-terminal domain containing the CXXC intersubunit disulfide isomerase motif; FP, fusion peptide; NH, N-helix; CX6CC, disulfide loop region; CH, C-helix; MPER, membrane proximal external region; TMD, transmembrane domain; CT, cytoplasmic tail. Domain abbreviations specific for HIV-1 gp; C1-C5, conserved domains 1 to 5; V1-V5, variable domains 1 to 5; CX5C, disulfide loop region. Intersubunit disulfides are indicated. The atomic structure has been determined for those regions colored gray. Panel B is modified from M. Caffrey (2011) Trends in Microbiology Vol.19 No4. 191-197.

1.4.1 THE MLV PERIPHERAL SUBUNIT, SU.

The MLV SU can be divided into three different functional domains, the N-terminal receptor binding domain (RBD), the flexible proline rich region (PRR) and the C-terminal domain (CTD) (Fig 6). RBD consists of about 245 amino acids and contains the binding site for the host cell receptor. This has been shown for the ecotrophic Friend-MLV (Fr-MLV) by producing this region as a soluble protein and testing its ability to bind to mCAT1, the host cell receptor. The binding was measured both directly using radio labelled proteins and indirectly testing the ability of RBD to interfere with Fr-MLV infection (Davey et al., 1997; Davey et al., 1999). The structure of the Fr-MLV RBD has been determined at 2Å resolution. It has a bent finger-shaped structure were the base consists of an anti-parallel β-sandwich and the tip, highly variable among gammaretroviruses, consists of two α-helical regions connected by loops (Fig. 7). The receptor specificity of RBD is determined by the variable regions. Mutagenesis, especially of residues Ser84 and Asp86, in one variable region of Fr-RBD leads to disruption of the interaction with the receptor and loss of infectivity (Davey et al., 1999). A second receptor binding site has also been suggested, on the opposite side of the molecule at residue Trp142 (Fig 7) (Zavorotinskaya and Albritton, 1999).

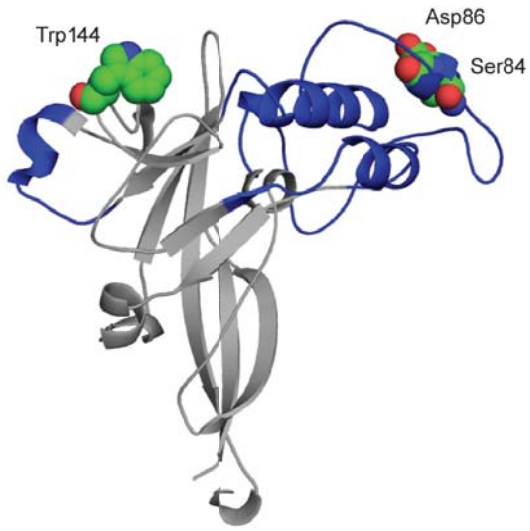

Fig 7. Structure of Fr-RBD (PDB ID code: 1AOL). Residues in the two receptor-binding sites are shown as spheres, the anti-parallel β-sandwich base is colored grey and the variable regions blue.

How does receptor binding activate the MLV spike for membrane fusion? Some important clues to this question have been achieved by studying an Env mutant with a deletion of His 8 (ΔH8). The His 8 residue belongs to a conserved SPHQ sequence in

the N-terminal region of SU. The ΔH8 Env mutant is correctly processed and incorporated into virus particles. It also binds normally to receptors but it cannot complete the membrane fusion process (Bae et al., 1997). However, the infectivity of the receptor bound mutant virus can be rescued by adding soluble RBD of wt SU *in trans* (Lavillette et al., 2000). Thus, after receptor binding the mutant RBD makes a loose enough interaction to the rest of the spike that it can be replaced by receptor bound wt RBD, which can activate the spike. Indeed, it proved possible to delete the entire RBD and still rescue some fusion with soluble RBDs as long the receptor was present. The fusion was significantly enhanced if the membrane contact of the RBD deleted spike was restored, by replacing the RBD with the hormone erythropoietin, which is known to bind to the erythropoietin receptor. Apparently, the wt RBD becomes activated by receptor binding to interact with the CTD of the defective SU in a way that triggers fusion. The interaction has been suggested to involve a region in the major disulfide loop of the CTD (Barnett and Cunningham, 2001; Barnett et al., 2001; Lavillette et al., 2001). However, in the native spike it is important that the RBD maintains a type of interaction with the CTD, which suppresses TM activation. The stability of this interaction is crucial in preventing premature spike activation. One important factor stabilizing the native spike structure seems to be the PRR. This region is positioned in between the RBD and the CTD and contains a stretch of about 45 amino acids that are unusually rich in proline residues. It has been documented that PRR mutants can cause efficient spike mediated cell-cell fusion although the virus particles were noninfectious. The reason seemed to be decreased spike stability resulting in spike activation for fusion before being incorporated into virus particles (Lavillette et al., 1998; Weimin Wu et al., 1998; Lavillette et al., 2002).

But how is then TM activated by the RBD triggered CTD? The TM is disulfide linked to the CTD. This disulfide bridge originates in SU from a conserved redox acive isomerase motif (Fig 6 and 8.) containing two cysteines interspaced by two other residues (Cys-X-X-Cys, CXXC). One of the Cys residues in the motif carries a free thiol-group and the other is engaged in the disulfide bridge (Pinter et al., 1997; Opstelten et al., 1998). The CXXC motif controls MLV fusion by inducing isomerization of the intersubunit disulfide. Thus, upon receptor binding the reactive thiol group within the CXXC motif attacks the intersubunit disulfide bond causing its isomerization to a CXXC disulfide bridge. This leads to the dissociation of SU releasing the fusion potential stored in TM. According to the prevailing model the receptor activated RBD changes the locale of the CXXC thiol through its altered interaction with the CTD so that the thiol becomes deprotonated and can attack the intersubunit disulfide (Li et al., 2007). Interestingly, the free thiol-group in the CXXC motif becomes exposed, upon receptor binding, before the disulfide rearrangement. By adding an alkylator during fusion activation the free thiol group can be alkylated and is then not able to rearrange the disulfide bond between SU and TM. This traps the spike in an intermediate structure, an isomerization arrested stage (IAS), which can be reactivated by artificial reduction of the intersubunit disulfide using e.g. DTT. It was also shown

that it was possible to activate the spike *in vitro* by chelating Ca^{2+} from the spike with EDTA or by pertubing the spike structure nonspecifically with heat, urea or guanidinium hydrochloride. Thus it became possible to convert all of the spikes to the IAS intermediate form in a virus preparation, using Ca^{2+} depletion *in vitro*, without the need for receptor interaction (Wallin et al., 2004, 2005).

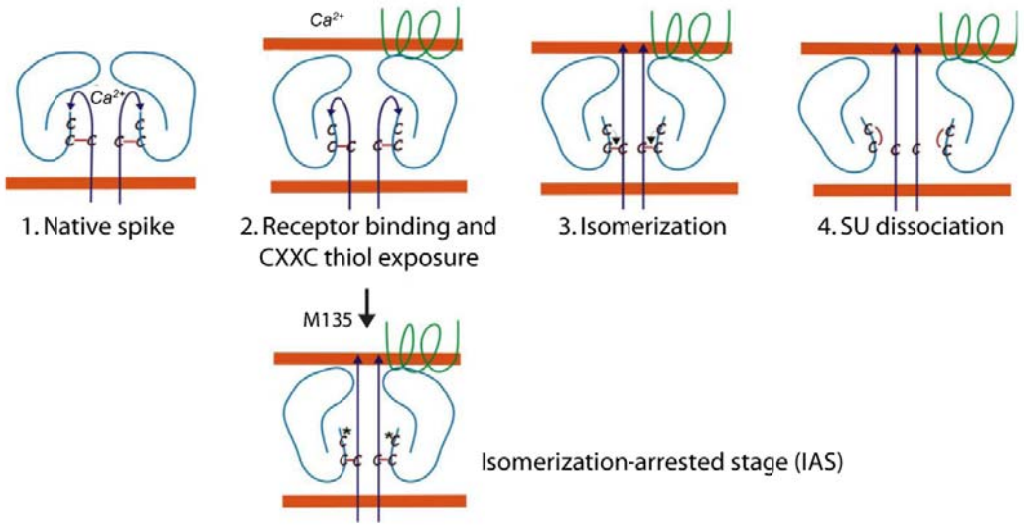

Fig 8. Schematic model for SU-TM disulfide bond isomerization during fusion activation of the MLV spikes. Each panel shows two of the three SU (light blue)-TM (dark blue) complexes that form one viral spike. The arrow indicates the location of the fusion peptide in TM. The SU contains a CXXC motif with one Cys disulfide-linked to TM and the other carrying a free thiol-group. (Panel 1) The native form of the spike is stabilized by Ca^{2+}. Panels 2-4 show how receptor binding activates a cascade of reactions starting with Ca^{2+} removal followed by CXXC-thiol exposure (panel 2), fusion peptide insertion into target membrane (panel 3), isomerization of the SU-TM disulfide-bond and SU dissociation (Panel 4) and finally TM-back-folding mediated membrane fusion (not shown). Shown is also the CXXC-thiol alkylated and isomerization-arrested stage, captured in the presence of an alkylator, e.g. 4-(N-maleimido)benzyl-trimethylammonium iodide (M135), during fusion activation (lower panel).

The structures of solubilized native and *in vitro* activated IAS spikes of Mo-MLV have been solved at 18 Å using single particle cryo-electron microscopy (cryo-EM). The reconstruction of the native structure showed a cage like trimeric structure with three prominent protrusions in each protomer, a top, middle and a lower protrusion (Fig 9). The top protrusion was curved as a bent finger towards the three-fold axis in the upper

part of the spike forming a roof to the spike cavity. The middle protrusion was located on the side making three side lobes in the trimeric spike and the lower protrusion formed three legs at the bottom. The crystal structure of RBD fitted well into the density of the top protrusion, defining this domain as the head of the spike. The corresponding protomer with the three protrusions was also found in the reconstruction of IAS spike structure, but drastic changes, particularly in the head region were observed. The curved finger-like protrusions did not point toward the center as in the native structure, but their tips appeared to have rotated to the periphery opening up the central cavity from above. The length of the middle protrusion was slightly reduced and the densities for the lower protrusion moved closer to the three-fold axis. It was speculated that the outward rotation of the RBD generated the signal to the CTD that subsequently activated TM for fusion. The open roof could make space and guide, a TM pre-hairpin intermediate towards the cell membrane (Wu et al., 2008).

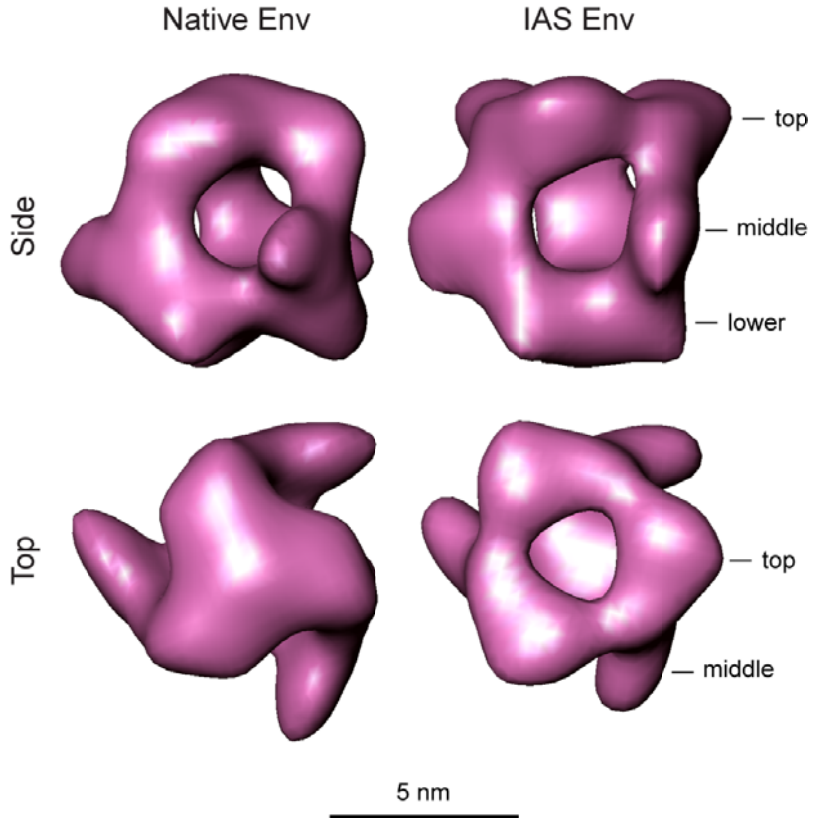

Fig 9. Side and top views of the surface rendered cryo-EM reconstruction of native (left) and IAS (right) spike trimers. The three protrusions are indicated. The scale bar represents 5 nm. In particular, note the opening of the cavity from above after activation of the native spike into the IAS form.

1.4.2 THE HIV-1 PERIPHERAL SUBUNIT, GP120.

The HIV spike is a trimer of the peripheral gp120 subunit and the transmembrane gp41 subunit. In contrast to MLV the subunits of HIV are not linked by a disulfide. The HIV-1 gp120 is divided into five variable (V1-V5) and five constant (C1-C5) regions (Fig 6). The spike activation process is initiated when gp120 binds to CD4. This interaction induces conformational changes in gp120 that exposes and forms the coreceptor binding site, which is specific for the chemokine receptor CCR5 or CXCR4. Coreceptor binding to the CD4 activated gp120 is believed to weaken the interaction between gp120 and gp41, activating the latter for fusion (Sattentau and Moore, 1991).

Several different crystal structures have been solved for the HIV gp120 (Kwong et al., 1998; Huang et al., 2005; Zhou et al., 2007; Pancera et al., 2010). All of these proteins have been expressed as monomers. They all have large deletions, usually removing the V1-V2 and V3 variable loops and the flexible N- and C-terminal ends. These engineered proteins are referred as the gp120 core. Furthermore, the different core structures are stabilized by bound antibody Fabs and soluble CD4 fragments. The structures are overall similar but clear differences are seen when comparing the complexes. The first gp120 core structure to be solved using X-ray crystallography was in complex with CD4 and Fab 17b. The gp120 core showed a heart-like structure composed of an inner- and outer-domain connected by a bridging sheet (Fig 10, panel A) (Kwong et al., 1998). The inner domain was believed to interact with gp41 at the three fold axis of the trimeric spike whereas the heavily glycosylated outer domain with the CD4 binding site was thought to be exposed on the surface (Kwong et al., 1998).

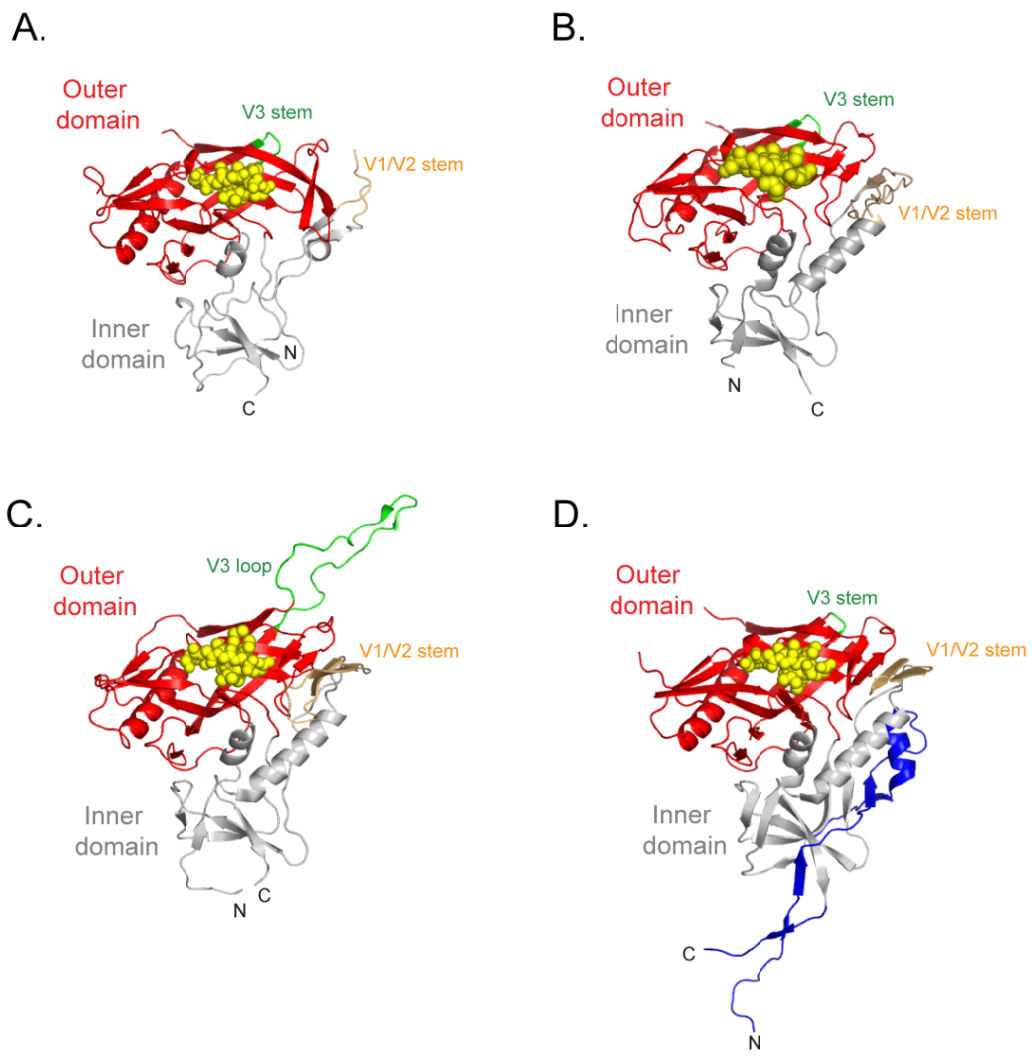

Figure 10. Structures of the HIV-1 gp120 core. (A) The atomic structure of gp120 core, derived from its complex with the b12 Fab (PDB ID code: 2NY7). This structure is believed to represent a close to native gp120 conformation. (B) The atomic structure of the gp120 core from its complex with CD4 and the 48d Fab (PDB ID code: 1GG1). This gp120 structure should be representative of the CD4 liganded conformation. (C) The atomic structure of the gp120 core with intact V3 loop, derived from its complex with the X5 Fab and CD4 (PDB ID code: 2B4C). This structure shows the conformation of the V3 loop believed to interact with the coreceptor. (D) The atomic structure of the gp120 core with the intact N- and C-terminal regions, derived from its complex with CD4 and 48d Fab (PDB ID code: 3JWD). The outer and inner domains are colored red and grey, respectively. The CD4 binding loop (residues 364-374) is colored yellow and shown as a spheres representation. The stub of the V1/V2 loops is orange, whereas the V3 stem and V3 loop are colored green. The N- and C-terminal regions are colored blue.

The structure of gp120 core protein in complex with the broadly neutralizing antibody b12 has also been solved (Zhou et al., 2007). This gp120 core had five engineered disulfides and four substitutions in the CD4 binding site cavity to restrict interdomain movements and to stabilize the bridging sheets. This structure also displayed a heart like structure and the outer domain was almost identical compared to the CD4 bound structure. However, the region forming the bridging sheet in the CD4 bound structure, formed in the Fab b12 complex two β-sheets and a loop instead. Also there were some differences in the inner domain close to the bridging region. It was suggested that the b12 stabilized gp120 core structure resembled an unliganded spike and that CD4 binding induced the formation of the bridging sheet (Zhou et al., 2007).

Biochemical studies have shown that the bridging sheet and the V3 loop constitute the binding site for the coreceptor. Furthermore, the data suggested that the V1-V2 loops cover the V3 loop in the native spike and that CD4 binding causes displacement of V1-V2 loops and exposure of the V3 loop for coreceptor binding (Sattentau and Moore, 1991; Thali et al., 1993; Wyatt et al., 1995; Sullivan et al., 1998; Sanders et al., 2000).

The structure of the gp120 core containing an intact V3 loop was solved in complex with CD4 and the Fab X5. This showed the same core structure as the other CD4 bound complex but the V3 loop formed a 30Å extension from the top of the gp120 core. Binding of gp120 to cell surface CD4 would position V3 so that its coreceptor binding tip points towards the target membrane (Huang et al., 2005).

The gp120 core structure including stabilizing T257A and S375W substitutions and almost intact N- and C-terminal ends was most recently solved. This structure was complexed with CD4 and the Fab 48d. Again a similar CD4 bound gp120 core structure was seen and the N- and C-termini made a 30Å extension pointing downwards from the core toward the viral membrane (Pancera et al., 2010). In a related publication it was proposed that the N/C-extension interacted with gp41 as suggested by mutational studies. Furthermore, it was speculated that when both CD4 and the coreceptor binds to the outer domain of gp120 a conformational shift occurs and that this transfers an activation signal via the inner domain to the N/C-extension, regulating the interaction with gp41 and its fusion activity (Finzi et al., 2010).

A vaccine that targets gp120 could potentially block the infection, as in the case of influenza virus (Karlsson Hedestam et al., 2008). However, the production of a vaccine against HIV-1 has so far been unsuccessful and it has been suggested that the structural flexibility of gp120 is the reason. It has been shown using thermodynamic measurements that CD4 binding to gp120 causes large changes in its enthalpy and entropy. This was interpreted as a considerable conformational flexibility in gp120 and that CD4 binding caused extensive structural rearrangements into a more stabile structure. This flexibility is probably needed during fusion activation and is also an advantage for the virus to avoid the immune system (Myszka et al., 2000). One

mechanism for gp120 to evade an immune response has been described as conformational masking of epitopes. This means that many antibodies formed against gp120 has difficulties in finding its epitope due to the conformational flexibility of gp120. Two exceptions have been found, b12 and VRC01, which are targeting the CD4 binding site. These antibodies do find their epitopes without causing significant structural alterations of gp120 (Chen et al., 2009; Zhou et al.).

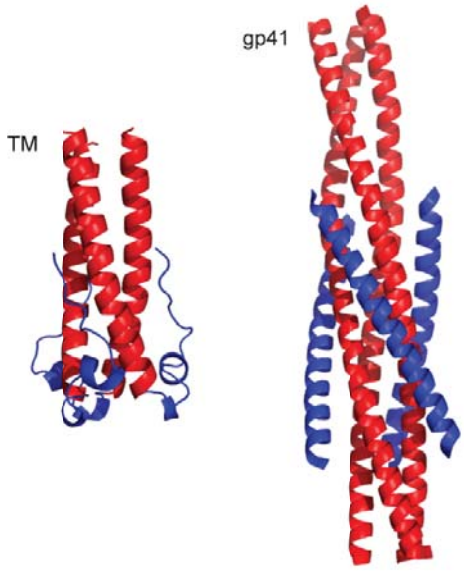

Fig 11. The "trimer of hairpins" or "six helical bundle" structures of the transmembrane subunit of MLV (left, PDB ID code: 1MOF) and HIV-1 (right, PDB ID code: 1ENV). The N-helixes (red) form a central coiled-coil-core onto which the C-terminal parts (blue) are packed.

1.4.3 THE TRANSMEMBRANE SUBUNIT OF MLV AND HIV-1.

The ectodomain of the transmembrane subunit.

The transmembrane subunit of MLV and HIV has many similarities and will be covered together in this section. This subunit includes an N-terminal fusion peptide containing 10-15 hydrophobic amino acid residues. It is believed that the fusion peptide is buried within the spike trimer structure and it is only exposed upon receptor binding. The direct involvement of the fusion peptide in membrane fusion has been confirmed by several mutational studies (Bosch et al., 1989; Freed et al., 1992; Schaal et al., 1995; Zhu et al., 1998). Downstream of the fusion peptide is a region predicted to form an amphipathic α -helix (the N-helix) (Fig 6). Further downstream is a second region also

predicted to form an α-helix (the C-helix) closer to the viral membrane (Fig 6). Peptides covering the N-helix and parts of the C-helix region have been crystallized and shown to form a trimeric N-helical coiled coil structure with the C-termini bent, like in a hairpin, interacting with the grooves of the N-helical coiled coil (Fig 11) (Fass et al., 1996; Chan et al., 1997; Weissenhorn et al., 1997). These structures resembled the post-fusion structure of the Influenza HA2. This supported an Influenza HA2-like fusion model where the N-helix of the transmembrane subunit is believed first to form an extended trimeric coiled coil (prehairpin) inserting the fusion peptide into the target membrane. Subsequently, the C-helixes fold into the grooves of the N-helical coiled coil forming a six helical bundled structure. This brings the target membrane and the viral membrane together for fusion. The model is supported by studies where parts of the N-helix or especially the C-helix has been added in peptide form to activated spikes of cell bound virus and shown to inhibit virus fusion (Jiang et al., 1993; Chan et al., 1998; Furuta et al., 1998). Importantly CD4 and coreceptor interaction is needed for peptide binding in the case of HIV-1, suggesting, that the peptides only binds to a spike intermediate structure e.g. the gp41 prehairpin (Furuta et al., 1998; Abrahamyan et al., 2003). Similarly, in the case of MLV it has been possible to bind fusion inhibiting TM peptides to IAS spikes, but not to native spikes (Wallin et al., 2006). However, it should be stressed that there is no structural data yet to support the existence of a prehairpin intermediate of the transmembrane subunit during retrovirus spike activation.

In between the N-helix and the C-helix of the transmembrane subunit is the chain reversal region. This region is part of the hinge in the back-folded post-fusion crystal structures of this subunit. Closely downstream of the hinge MLV TM contains a conserved CX_6CC motif. This is, with the last Cys of the motif, making the disulfide bond to the isomerization motif in SU (Pinter et al., 1997; Opstelten et al., 1998). The other two Cys residues of the motif are linked internally and therefore the region has also been called the disulfide loop region. It is interesting that the CX_6CC motif is conserved among gamma retroviruses, delta retrovirus including HTLV, alfa retroviruses including ALV and also filoviruses including Ebola virus (Delos et al., 2010). In the case of ALV and Ebola virus the motif is disulfide linked to SU, but the Cys in SU is not part of an isomierization motif. However, in the case of HTLV the SU Cys is part of an isomerization active CXXC motif (Li et al., 2008). These well conserved Cys residues in TM suggest a common function for this region in interacting with SU and also in controlling TM activation. Mutations inserted into the chain reversal region has also been shown to inhibit membrane fusion due to possible defects in back-folding (Maerz et al., 2000; Delos et al., 2010).

HIV-1 contains a CX_5C motif in the corresponding region of gp41. This is conserved among the lentivirus group. However, HIV-1 lacks the CXXC motif in gp120 as well as the intersubunit disulfide bridge. Nevertheless, the CX_5C region is also known to interact with gp120 in the native HIV-1 spike. If the CX_5C motif in gp41 is engineered into a CX_5CC motif, this extra Cys can make a stable disulfide bond to a Cys introduced

in the C-terminal region of gp120 (Binley et al., 2000). This mutant is known as HIV-1 SOS. Conformational changes within this spike mutant upon CD4 and coreceptor binding allows DTT mediated reduction of the disulfide bond, rescuing membrane fusion (Abrahamyan et al., 2003; Binley et al., 2003). Thus, the HIV-1 SOS can be used for trapping a receptor activated intermediate structure of the spike.

The membrane proximal external region (MPER).

The MPER is positioned immediately external to the viral membrane and contains about 20-25 amino acids, many of which are Trp residues. The MPER has been extensively studied in the case of HIV-1. The peptide structure of the MPER has been determined but unfortunately this is in dispute. In one recent study it was shown that the MPER peptide was an L-shaped molecule with two amphipathic α-helixes separated by a hinge. The hydrophobic sides of the helixes were inserted into the viral membrane (Sun et al., 2008). MPER peptides have also been observed in the form of an extended β-turn and it has been suggested that both conformations exist but in different functional states of the spike (Ofek et al., 2004). In the trimeric spike the MPERs have been modeled to extend from a common TM stem along the membrane surface to the periphery.

Deletions or substitution of amino acids within the MPER of viral spikes have been shown to affects viral fusion (Munoz-Barroso et al., 1999; Salzwedel et al., 1999). MPER peptides also bind to membranes and cause membrane leakage, like isolated fusion peptides do (Suarez et al., 2000a; Suarez et al., 2000b). These findings suggest that MPER has an active role in the membrane fusion reaction.

The MPER is interesting for immunological reasons because two rare, broadly neutralizing, antibodies against HIV-1, 2F5 and 4E10, bind to this region. Surprisingly, these antibodies do not bind to native spikes but find their epitopes first after fusion activation (Ofek et al., 2004; Dimitrov et al., 2007; Alam et al., 2009). In addition it has been found that 2F5 and 4E10 has week affinity for membranes and that this ability is vital for their neutralizing effect. It was suggested that the membrane affinity concentrated 2F5 and 4E10 to the virus membrane, taking them into close proximity of the MPER and allowing quick epitope binding upon fusion activation (Alam et al., 2009). NMR has been used to determine the structures of 2F5 and 4E10 Fab bound MPER. These showed that both antibodies bound the L-shaped peptide at the membrane interface and disrupted the structure of the hinge region between the two helices. It was speculated that the MPER hinge was vital for fusion and that 2F5 and 4E10 block this function (Song et al., 2009).

The membrane spanning domain

The transmembrane domain (TMD) is composed of about 22 amino acids. One major function is to anchor Env to the lipid bilayer. However, the TMD is one of the most conserved parts of retrovirus Envs suggesting additional functions. In the case of HIV-1 it has been shown that a GGXXG motif in the TMD is important for membrane fusion (Shang et al., 2008; Shang and Hunter, 2010). In bacteria a GGXXG motif has been suggested to be important for associations between transmembrane domains (Senes et al., 2004). Perhaps, GGXXG mediated interactions are involved in the viral fusion process. The GGXXG motif is not present in MLV, but it has been shown that a Pro residue in the TMD is important for fusion (Taylor and Sanders, 1999).

The cytoplasmic tail

All viral fusion proteins have a CT which can vary a lot in size, i.e. the CT of influenza HA contains 11 amino acids that of, MLV Env 32 amino acids and CT of the HIV-1 gp about 150 amino acids. Although the size variance is huge, they all have similar functions. The CTs are needed to interact with cellular and/or viral proteins that direct intracellular transport of the fusion protein and its incorporation into virus particles. For instance the unusually long CT of the HIV-1 spike binds to TIP47, which is needed for efficient spike incorporation into particles (Blot et al., 2003; Lopez-Verges et al., 2006). In addition the CT in most viral fusion proteins has been shown to control the fusion activity. The mechanism behind this is an important, but unresolved question.

A good model system to study the function of the CT during membrane fusion was found in MLV where the viral PR, during virus particle maturation, cleaves the 16 amino acids long R-peptide from the cytoplasmic tail of TM (Green et al., 1981; Henderson et al., 1984). The processing has been shown to be critical for the viral fusion function. This was shown by expressing full length Env and R-peptide deleted Env in cells and finding that the deleted Env caused membrane fusion between cells (Ragheb and Anderson, 1994; Rein et al., 1994). Thus, TM with the R-peptide represents a precursor form of Env which protects it from premature fusion activation, which is potentially harmful for the producer cell. During virus release the viral protease cleaves the R-peptide and activates the fusion potential in TM. The R-peptide cleavage is a conserved event among gammaretrovirus and has also been reported for the β-retrovirus, MPMV, and the lentivirus, equine infectious anemia virus (Rice et al., 1990; Brody et al., 1994; Bobkova et al., 2002). It is not known how the R-peptide restrains membrane fusion, but several models have been suggested. Firstly, the R-peptide has been shown to be palmitoylated and it has been suggested that this targets the R-peptide to the inside of the plasma membrane, suppressing fusion (Olsen and Andersen, 1999). Secondly, It has been suggested that a host cell protein interacts with the R-peptide suppressing membrane fusion (Yang and Compans, 1997). However, no such protein

has been found so far. Thirdly, the R-peptide trimer in the spike has been suggested to form a helical coiled-coil structure stabilizing the spike in its mature, fusion suppressing state. This is supported by secondary structure modeling and mutations introduced to regions believed to stabilize the helical coiled-coil (Taylor and Sanders, 2003). Such destabilizing mutations rescued fusion in Env with R-peptides.This third model is also supported by the results of a study with the paramyxovirus fusion protein. In this a stabilizing trimerization motif was inserted into the C-terminal end of the transmembrane subunit and it was found that this restricted its folding into the six helical structure upon activation. It was speculated that that CT trimerization prevented rotations in the plane of the membrane making it impossible for the C-helix region to back fold into the grooves of the trimeric N-helical coiled-coil (Waning et al., 2004).

Some more hints to the mechanism by which the R-peptide exerts its function in the MLV spike was achieved by biotinylation and epitope mapping of the spike surface. It was found that R-peptide cleavage induced significant changes in the spike ectodomain (Aguilar et al., 2003). Finally, video fluorescence microscopy and electrical capacitance measurements have been used to investigate the formation of fusion pores created by the MLV spikes with and without the R-peptide. It was shown that R-peptide containing spikes were unable to create fusion pores on receptor positive host cells. It was concluded that the R-peptide suppresses spike mediated fusion before the lipid mixing and hemifusion stage (Melikyan et al., 2000).

In HIV-1 the long CT of the spike has been shown to affect fusion in many ways. First, deletions of the spike CT has been shown to increase fusion efficiency of the virus (Edwards et al., 2002; Wyss et al., 2005). Secondly, using immature particles with uncleaved Gag it has been shown that the spike CT interacts with the Gag layer below the membrane and that this suppresses the fusion function of the spike. Deletion of the CT releases this block (Davis et al., 2006; Wyma et al., 2004; Wyma, Kotov, and Aiken, 2000). Thirdly, an interesting observation has been that HIV-1 treated with a cholesterol binding compound that blocks virus entry, amphotericin B methyl ester (AME), quickly developed resistance. This was shown to be caused by a single amino acid substitution leading to cleavage of the CT by the viral PR (Waheed et al., 2007; Waheed et al.). Interestingly, no stop codon deletions of CT were observed. Given that the viral protease is active during or soon after budding this suggests that the full length of the CT was needed for synthesis, transport and gp incorporation. However, the CT cleavage was favorable for the virus particle upon fusion. It is possible that AME stabilizes the gp trimer in its native prefusion state or restricts spike mobility in the membrane, which is needed for fusion activation, and that CT cleavage releases this fusion inhibitory effect.

1.4.4 THE STRUCTURE OF THE RETROVIRUS SPIKE

The first structure of a retrovirus spike was reported for MLV in 2005. This was resolved using the combination of cryo electron tomography of virus particles and single particle analysis of spike subvolumes. The native MLV spike was found to carry multiple projections in its head region and it was standing on the membrane with tripod legs (Forster et al., 2005). In 2006 there were two different structures published on the native spike of Simian immunodeficiency virus (SIV). The spike in these studies contained a truncated CT to increase spike incorporation into virus particles (Zanetti et al., 2006; Zhu et al., 2006). However, even though similar methodology was used the final structures were very different from each other. Zhu et al. presented a structure with a compact head standing on three legs and Zanetti et al. showed a mushroom like spike structure with a compact head connected to the viral membrane by a stalk suggested to contain gp41. The first 3D reconstructions of native and CD4 bound HIV-1 spike structures were reported by the group of Subramaniam in 2008 (Liu et al., 2008). The unliganded spike in this study represents today's paradigm of the in situ HIV spike structure. This contained a hollow head connected to the viral membrane by a compact stem. In the head region the protomeric units formed blade-like lobes on the sides and interprotomeric connections at the three fold axis at top. The atomic structure of the gp120 core from its complex with b12 Fab could be fitted into the lobe, such that the stems of the truncated V3 and the V1-V2 loops pointed toward the top of the head. The putative gp41 binding region of the gp120 core inner domain was pointing towards the lower parts of the head. The known glycosylation sites were all exposed to the external side and the CD4 binding region was located on the concave side of the lobe. In this way the fitting of the core gp120 structure validated part of their head structure (Liu et al., 2008). However, the crystal structure of gp120 core including its N- and C-terminals did not fit into their spike structure (Pancera et al., 2010). In particular the N/C extension known to interact with gp41 was located outside the stem, questioning this part of the EM structure. CD4 binding to the spike in the virus could not be studied without the stabilization of the complex with the 17b Fab. It was observed that the CD4 and Fab binding caused a significant rotation of the gp120, which opened up the roof of the cavity in the head. This was suggested to facilitate the interaction of the gp41 prehairpin with the cell membrane.

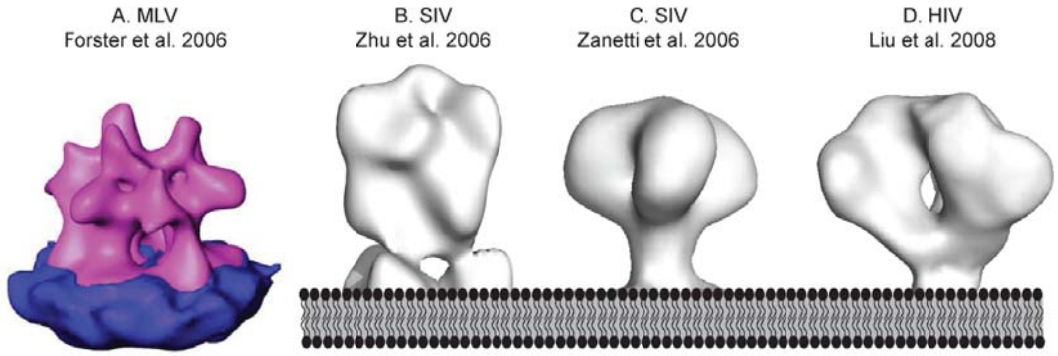

Fig 12. Cryo-electron tomographic reconstruction of native retrovirus spikes. (A) The Mo-MLV spike model of Forster et al. with multiple head projections and tripod legs (copyright permission (2011) from National Academy of Sciences, U.S.A.). (B) The SIV spike model of Zhu et al. with a compact head and tripod legs. (C) The SIV spike model of Zanetti et al. with a mushroom like spike appearance. (D) The HIV-1 spike model of Liu et al. with a hollow head connected to the viral membrane by a compact stem.

2. AIMS OF THE STUDY

Retroviruses incorporate their genome into the host cell DNA and once the cell becomes infected it will continue to be so during its existence. Thus, a strategy towards an absolute prevention of retrovirus infection is to block the virus before it enters the cell by membrane fusion. I am trying to understand the structural transitions of the retrovirus fusion protein during fusion activation. This will increase the chances to find a definite prevention against retroviral infections.

The aims of this study have been to find out:

- If the intersubunit disulfide bond isomerization between SU and TM of MLV represents a receptor activated event that is necessary for virus induced membrane fusion (paper I).
- If the R-peptide cleavage of MLV Env is needed for the SU-TM disulfide isomerization reaction (paper II).
- How the R-peptide cleavage is synchronized in MLV Env trimers (paper III).
- The structure of native HIV-1 gp trimer and its conformational changes upon CD4 receptor binding (paper IV).

3. MATERIAL AND METHODS

3.1 CELLS

Human embryonic kidney 293T cells were maintained in Dulbecco's modified Eagle's medium (DMEM) containing 4.5 g/liter glucose (Invitrogen, Paisley, UK) supplemented with sodium pyruvate, nonessential amino acids (Invitrogen), L-glutamine, and 10% fetal calf serum (FCS). The XC cells originated from a Rous sarcoma virus induced rat tumor and were maintained in DMEM containing 1 g/liter glucose (Invitrogen) supplementaed with L-glutamine, and 10% FCS. The NIH 3T3 mouse embryonic fibroblast cells (3T3) were maintained in DMEM containing 4.5 g/liter glucose supplemented with L-glutamine, and 10% FCS. The MOV-3 cell line is a 3T3 cell line that is chronically infected by Mo-MLV. This was obtained from G. Schmidt, GSF-National Research Center for Environment and Health, Neuherberg, Germany. The MOV-3 cells were maintained as the 3T3 cell line.

3.2 ANTIBODIES

The anti R-peptide antibody, αR, is an affinity-purified polyclonal antibody from rabbits immunized with a 17 amino acids long peptide corresponding to the Mo-MLV R-peptide, NH_2-CVLTQQYHQLKPIEYEP-$CONH_2$. An extra Cys was added to the N-terminus as a conjugation site (Innovagen, Lund, Sweden). The Mo-MLV-specific rabbit antiserum, αMLV (HE863), and the Mo-MLV SU-specific rabbit antiserum, αSU (HE699), originated from Viromed Biosafety Laboratories, Camden, NJ. The antibody against the influenza of HA tag (YPYDVPDYA) was from Roche (Basel, Switzerland). The HIV-1 17b monoclonal antibody targets a CD4 induced epitope in gp120 and originate from NIH AIDS research and reference reagent program: From James E Robinson.

3.3 REAGENTS OF SPECIAL ATTENTION

N-Ethylmaleimide (SIGMA-Aldrich Chemie, Munich, Germany) ***(NEM)*** is a membrane permeable alkylating reagents that binds covalently to free thiol groups (-SH), e.g. present in Cys residues. Cys residues in proteins can form disulfide bonds between their thiol groups (-S-S-). MLV SU contains an isomerase motif (CXXC), were one Cys is covalently attached to TM and the other carries a free thiol group. Upon spike activation the free thiol becomes exposed, attacking the SU-TM disulfide and isomerizes it to an intra CXXC disulfide bond (Fig 13, A-C). NEM is able to bind to the

exposed thiol before SU-TM isomerization, thus, trapping SU and TM in their covalently bound form (Fig 13, D).

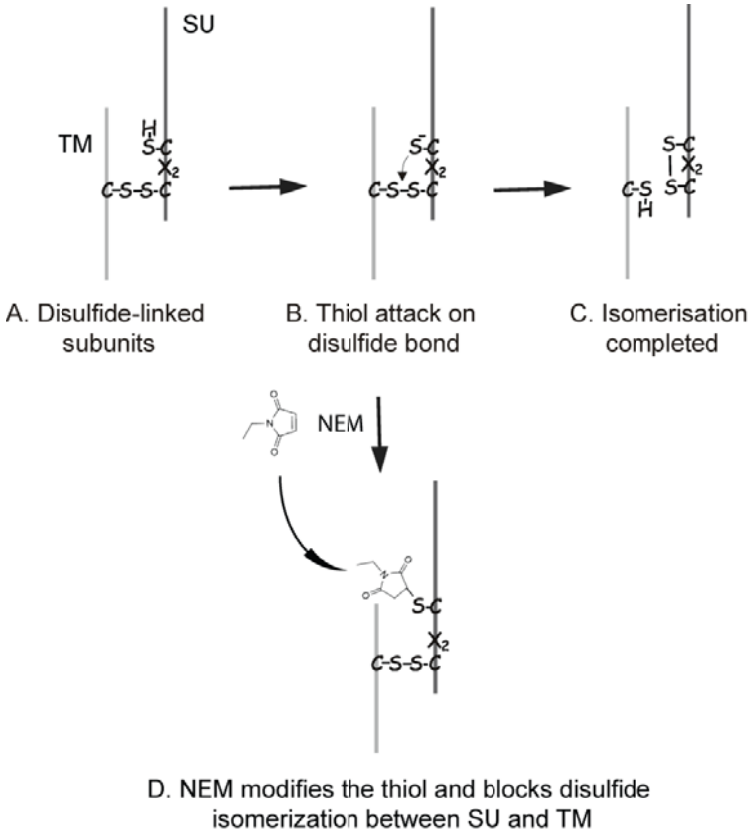

Fig 13. The mechanism of MLV SU and TM disulfide bond isomerization and the effect of NEM.

4-(N-maleimido)benzyl-trimethylammonium iodide (Toronto Research Chemicals Inc., North York, Canada) ***(M135)*** is a membrane impermeable variant of NEM. M135 was used in some experiments to alkylate viral spikes that become receptor activated upon incubation of virus with host cells. An advantage with M135 is that it can be washed away after incubation of virus with cells, which is not possible for a membrane permeable alkylating reagent like NEM. M135 is also less toxic for cells than NEM.

Dithiothreitol (SIGMA-Aldrich) ***(DTT)*** is a strong reducing agent that reduces disulfide bonds according to the mechanism shown in figure 14. DTT was used for reducing SDS-PAGE and also for artificial reduction of the disulfide between SU and TM in virus with an alkylated CXXC thiol.

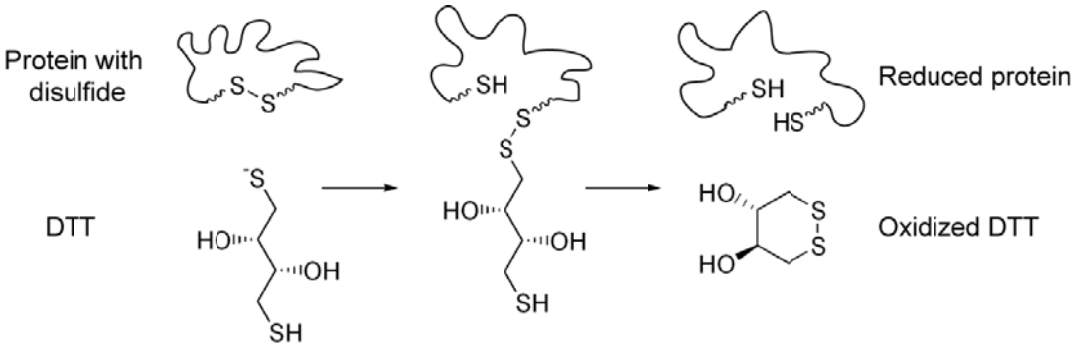

Fig 14. DTT reduction mechanism.

Chlorpromazine (SIGMA-Aldrich) ***(CPZ)*** is a drug that lowers the energy threshold needed for membrane fusion by facilitating conversion of the hemifusion stage into fusion pores. This effect has been used to determine whether an arrested fusion process has reached the state of hemifusion.

Amprenavir (obtained from the AIDS Research and Reference Reagent Program, Division of AIDS, NIAID, NIH) is a HIV protease inhibitor that binds to the active site of the protease. It was previously shown that amprenavir also inhibited the MLV protease activity and this notion was utilized to produce wt MLV particles with uncleaved R-peptides (Feher et al., 2006).

3.4 VIRUS PRODUCTION AND PURIFICATION

MOV-3 cells were used to produce Mo-MLV particles. Cells were grown in 75 cm^2 culture flasks to a confluence of about 90 %. Thereafter medium was changed to DMEM medium containing 5 % FCS and virus in medium was collected after 24 h, followed by a low speed centrifugation at 1,500 rpm for 15 min at 4 °C to remove cell debris. Virus-containing supernatant was layered on top of a step gradient composed of 1 ml of 60% and 4.5 ml of 20% sucrose (weight/weight) in HNC buffer (50 mM HEPES, 100 mM NaCl, 1.8 mM $CaCl_2$, pH 7.4,) and centrifuged at 4°C for 2 h at 22,000 rpm in a Beckman SW28.1 rotor. Virus was collected from the 20/60% sucrose

interphase. To produce radio labelled virus, 50 µCi/ml [^{35}S]-Cys was added to DMEM medium containing 5% FCS and depleted in Cys. Labelled virus was then purified as described.

To create mutated MLV the plasmid pNCA (obtained from Stephen Goff, Columbia University, New York, NY) encoding the full-length Mo-MLV genome was used. Two separate PCRs were performed to introduce the mutation into two overlapping DNA fragments and these were joined in a fusion-PCR. The mutated fragment was then cleaved by restriction enzymes and purified using a gel extraction kit, before ligation at 16 °C overnight with T4 DNA ligase into the correspondingly cleaved pNCA plasmid. *E.coli* JM109 were transformed with the ligated DNA for 30 min on ice. Thereafter the samples were heat-shocked at 37 °C for 30 seconds. The bacteria were seeded on LB-agar plates containing 50 µg/ml ampicillin and incubated overnight at 37 °C. Colonies were collected and screened using DNA sequencing. 293T cells were then transfected with 20 µg of the proviral DNA in a 75 cm^2 flask using calcium phosphate coprecipitation. Virus labeling and purification were performed as above.

To produce HIV-1 virus like particles (VLP), one 150-cm^2 flask with 293T cells was transfected with 20 µg pCAGGS JR-FL gp160 SOS ΔCT and 20 µg pNL4-3.Luc.R-E- (pNL) DNA using calcium phosphate coprecipitation. The gp160SOSΔCT DNA encodes the HIV-1 gp with an intersubunit disulfide and a gp41 endodomain deletion. The pNL DNA encompasses an HIV-1 genome with env and vif truncations, a frame shift mutation in the vpr gene and the luciferase gene in place of nef. VLP labeling and purification were performed as above.

For EM-analyses of HIV-1 spikes, ten 150-cm^2 flasks with 293T cells were transfected as described. VLPs were collected in the culture medium from 8 h to 48 h after transfection and then purified and concentrated in several steps at 4 °C. First, the medium (110 ml) was clarified by low-speed centrifugation for 10 min at 8 krpm in a JS13.1 rotor (Beckman Instruments, Brea, CA US). VLPs in the supernatant were purified by sedimentation in parallel step gradients, where 25 ml clarified medium was layered on top of 7 ml 20% (weight/weight) and 3 ml 60% (weight/weight) sucrose in HNC buffer (50 mM Hepes, 100 mM NaCl, 1.8 mM CaCl2, pH 7.4) and centrifuged for 2 h at 22 krpm in an SW 28 rotor. The 20%/60% interphases with VLPs were pooled and sucrose removed by overnight dialysis against 1 liter of HNC in 0.5-3 ml Slide-A-Lyzer cassettes (molecular weight cutoff, MWCO, 20 kDa) (Pierce, Rockford, IL USA). The sample was concentrated in an Amicon Ultra 15 (MWCO = 100 kDa) centrifugal filter device (Millipore, Billerica, MA US), to a final volume of about 100 µl. To isolate the spikes, samples were lysed in HNC buffer containing 2% TX-100 for 10 min at 37 °C and then subjected to sedimentation in a linear 5–20% (weight / weight) sucrose gradient, in HNC containing 0.05% TX-100, superimposed by a 0–0.2% (weight / weight) glutaraldehyde gradient, at 28 krpm for 18 h at 4 °C in a SW 55 rotor. The gradient was fractionated from the top into 13 fractions (50 µl), and analyzed by blue native (BN)-PAGE and silver staining. Sucrose was removed in a Zeba desalt spin

column (Pierce) for the fractions containing pure trimers. The sample was finally concentrated in a centrifugal filter device Microcon YM 30 (MWCO = 30kDa) (Millipore) and used for EM analyses.

3.5 SDS- AND BN-PAGE

Sodium dodecyl sulfate polyacrylamide gel electrophoresis (SDS-PAGE) is a method used to separate proteins according to their electrophoretic mobility. Since SDS binds to the entire polypeptide chain, samples end up with approximately identical charge per unit mass of polypeptide. Thus it is possible to separate proteins mainly due to size. The SDS-PAGE is not suitable for following protein complexes in the electrophoresis, because SDS efficiently disrupts noncovalent protein interactions. To follow protein complexes, i.e. HIV-1 spikes, the blue native polyacrylamide gel electrophoresis (BN-PAGE) protocol has been used. Commasie brilliant blue binds to protein complexes without disrupting them and provide the necessary charges for the electrophoretic separation.

3.6 MLV FUSION ASSAYS

There are two main assays, fusion-from-within and fusion-from-without, to follow the membrane fusion activity of viral spikes. The Fusion-from-within assay refers to the methodology where viral spikes are expressed in a cell line, in the absence of other viral proteins. The function of the spikes is then followed by mixing the spike expressing cells with cells expressing viral receptors. Spikes binds to receptors and membrane fusion take place between spike- and receptor-expressing cells (Fig 15, left column).

It is also possible to add virus particles to confluent cells that express the viral receptor. Some cell bound virus particles will be able to interact with two separate cells in close proximity to each other. Upon fusion, these virus particles will merge the membranes of the two cells together. This methodology is referred to as fusion-from-without (Fig 15, right column). With the fusion from without assay it is possible to follow the fusion of a synchronized activation of cell bond virus particles if the virus has been bond at 4 ˚C and then incubated at 37 ˚C. This is not possible with the fusion from within assay where spikes are continuously synthesized. The downside of the fusion-from-without assay is the low amount of fusion events compared to the fusion-from-within assay.

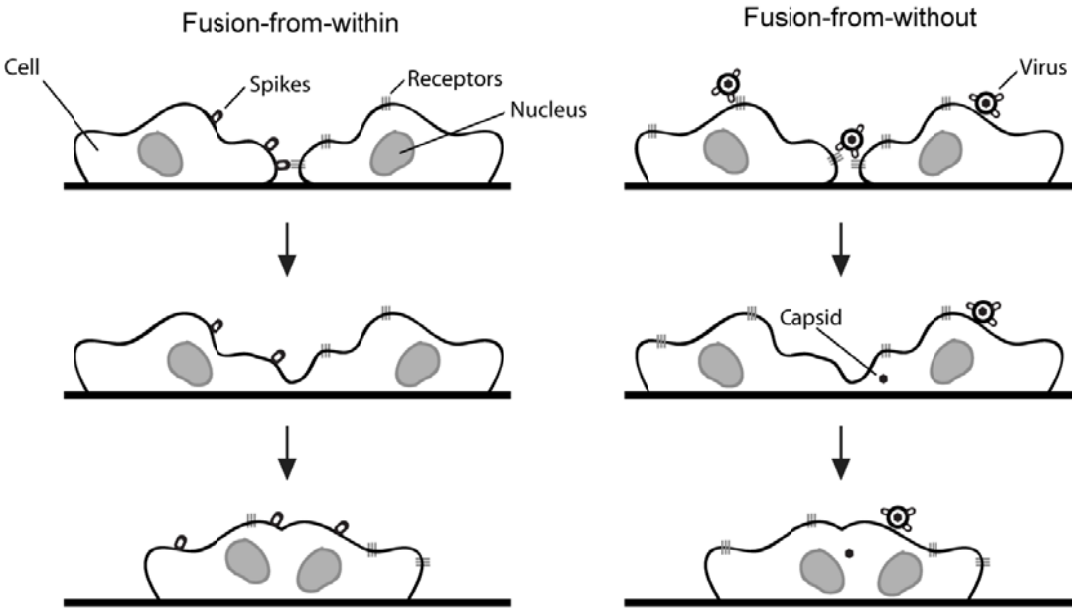

Fig 15. The principles of the fusion-from-within assay (left) and the fusion-from-without assay (right).

In this thesis the fusion-from-without assay has been utilized to analyze the fusion activity of Mo-MLV. To increase the amount of virus binding to cells Mo-MLV was sedimented onto XC cells by centrifugation, at 2900rpm for 1 h at 4°C, using a Beckman JS5.9 rotor, in HNC buffer containing 20 μg/ml polybrene. After this so called spinnoculation, the buffer was exchanged to prewarmed buffer (37°C) and the cultures incubated at this temperature for about 15 min to allow virus mediated cell-cell fusion. Thereafter, any remaining fusion active spikes were inactivated by treatment with an acidic buffer containing 40 mM sodium citrate, 10 mM KCl, and 135 mM NaCl, pH 3.0, for 1 min at room temperature. XC cell medium was added, and the cultures were incubated for 2 h at 37°C to let fused cells form polykaryons. These were visualized by staining with Giemsa (Sigma). To estimate fusion efficiency, we calculated the relative number of nuclei that were localized in polykaryons as a percentage of the total number of nuclei in the cultures. For each experiment five microscope fields (about 1,000 nuclei) of each sample were analyzed with the help of the ImageJ plug-in Cell Counter.

3.7 MLV SU AND TM DISULFIDE BOND ISOMERIZATION ASSAYS

MLV Env contains an intersubunit (SU-TM) disulfide bond which is coupled to a disulfide isomerase motif in SU. This motif is composed of two Cys residues separated by two other amino acids, CXXC. One of the Cys residues mediates the disulfide to TM

whereas the other carries a free thiol group (-SH) (Pinter et al., 1997; Opstelten et al., 1998). Upon receptor binding the free thiol in the CXXC-motif becomes exposed and activated to isomerize the SU-TM disulfide. The receptor mediated isomerization releases SU from TM, thus triggering the fusion activity of TM. If an alkylating agent is added during fusion activation this modifies the exposed thiol in the CXXC-motif before isomerization takes place and traps SU and TM in an isomerization arrested and disulfide linked stage (IAS). Notably, the native spike cannot be alkylated at this position, i.e. the IAS spike represent an intermediate form of the receptor triggered spike (Wallin et al., 2004).

In this thesis different kinds of SU-TM disulfide bond isomerization assays have been used and they are all depending on the finding that detergents such as NP-40 and Triton X-100 are strong inducers of SU-TM disulfide isomerization *in vitro*. If detergent is added to Mo-MLV and the mixture is incubated at 37˚C for 30 min, the intersubunit disulfide of all spikes rearrange and all SU-TM complexes dissociate and migrate separately as free SU and TM on nonreducing SDS-PAGE. If NEM is present during the detergent induced isomerization, SU and TM maintains the covalent bond and migrate as a SU-TM complex because the isomerization active thiol will be blocked by alkylation. In this way it was possible to follow the SU-TM disulfide bond isomerization reaction biochemically.

Receptor mediated isomerization of the intersubunit disulfide in the spike.

Purified radiolabelled Mo-MLV was diluted in HNC buffer containing 20 μg/ml polybrene and spinnoculated onto XC cells at 4 ˚C. Free virus was washed away and pre-warmed (37°C) HNC buffer was added. The cultures were then incubated for different times at 37 °C, allowing receptor induced activation of viral spikes for fusion-from-without. The virus-cell samples were then put on ice to stop the reaction. Thereafter, HNC buffer containing detergent and NEM was added and the samples incubated for 30 min at 37 °C. This treatment trapped all unactivated SU-TM complexes covalently together at the IAS. The amount of receptor induced SU-TM disulfide isomerization could be quantified in nonreducing SDS-PAGE by relating the amount of free SU to the amount of SU and TM in covalent SU-TM complexes.

Receptor mediated formation of spikes at the IAS.

Purified radio labelled MLV was diluted in HNC buffer containing 20 μg/ml polybrene and spinnoculated onto XC cells at 4 ˚C. Non-bound virus particles were washed away and pre-warmed (37°C) HNC buffer containing 2 mM M135 was added to initiate the fusion reaction. The cultures were then incubated for different period of times at 37 °C. At these conditions all receptor activated spikes will be trapped at the IAS. Samples

were put on ice to stop the reaction and then washed thoroughly to remove all excess of M135. HNC buffer containing detergent was added and the samples incubated 30 min at 37 °C. This isomierized the intersubunit disulfide in all SU-TM complexes that were not previously receptor activated and trapped at the IAS. The amount of spikes at the IAS was possible to quantify in nonreducing SDS-PAGE by relating the amount of disulfide linked SU-TM complexes to the amount of free SU.

In vitro triggering of the SU-TM disulfide isomerization reaction.

The MLV spike shows a very inefficient receptor independent isomerization of the intersubunit disulfide at 37 ˚C. This reaction can be much enhanced if the spike is Ca^{2+} depleted. Therefore, incubation of virus in Ca^{2+} free buffer provides conditions for an *in vitro* intersubunit disulfide isomerization reaction. This can be potentiated by increasing the pH of the buffer or if the Ca^{2+} chelating agent EDTA is included. Thus, purified radiolabelled Mo-MLV particles were diluted in HN buffer (pH 8.0) lacking Ca^{2+} and incubated for 0-5h at 37 °C, allowing *in vitro* isomerization of the SU-TM disulfide. Detergent and NEM was then added to the samples, followed by a 30 min incubation at 37 °C, to trap all unactivated spikes at the IAS. The samples were then analyzed by non-reducing SDS-PAGE. The amount of *in vitro* induced SU-TM disulfide isomerization was quantified by relating the amount of free SU to the amount of SU-TM complexes.

3.8 PROTEIN STRUCTURE DETERMINATION

3.8.1 ELECTRON MICROSCOPY VERSUS X-RAY CRYSTALLOGRAPHY AND NMR.

For structural determination of proteins there are several techniques to choose from, X-ray crystallography, nuclear magnetic resonance (NMR), single particle cryo-EM and cryo-EM tomography. The different methods all have their benefits and limitations. X-ray crystallography is the most commonly used method and it determines the arrangement of atoms inside a crystal structure by studying the diffraction patterns of X-rays. This method has been used to solve the structure for many different proteins at a resolution down towards 1Å. Limitations include the requirements of high protein concentration and purity, and the protein needs to form a well organized crystal for data collection. These organized crystals are rarely formed for larger proteins and protein complexes, due to structural flexibility and heterogeneity. NMR is another high resolution method to determine protein structures and it is based on isotope labeling, i.e. ^{13}C or ^{15}N. In a high magnetic field it is possible to track the isotope labelled atoms and calculate their positions in a 3D structure. NMR is very useful for proteins that do not form crystals and the main drawback is that it only works for relatively small proteins, usually smaller than 35 kDa. Thus, both X-ray crystallography and NMR do have downsides when working with large proteins and protein complexes. One strategy to circumvent these limitations has been to solve the structures of separate domains of larger proteins or stabilize the protein by deletions or by introducing structural modifications. This in turn raises questions about how these changes affect the structure of the protein.

Transmission electron microscopy (TEM) is the best suited technique to study the structure of intact protein complexes that are unable to form crystals. TEM can be divided into different approaches, single particle analyses and tomography. The principle of TEM includes the usage of free electrons that are discharged towards an ultra thin specimen and electrons passing through the sample are registered. This works much in the same way as light registers to a camera film. The advantage of using electrons is their short wavelength, compared to visible light, allowing smaller detailed to be visualized. One problem with exposing biological samples to doses of electrons is destruction of the sample. This has been solved either by using different stain techniques or freezing. Stains provide a protected shield over the organic tissue or protein sample. However, this severely limits detection of smaller details and also could destroy the native protein structure. To collect high resolution EM data and preserve the native protein structure, samples can be plunge frozen into liquid ethane causing water to form vitreous ice. This rapid freezing avoids ice crystals that otherwise destroys the sample. Data collected from vitrified samples need to be gathered during low electron dose not to demolish the organic sample. This method is known as cryo-EM. Using the single particle approach proteins are purified and vitrified in soluble form, and it is assumed that they obtain a random orientation in the sample. This is necessary to reconstruct the 3D structure of the particles from 2D particle images seen on the

micrographs. The information from one particle is limited and in general thousands up to hundreds of thousands of particles are selected. Thereafter, particles are classified into groups of images with the same appearance. The average density of each class is then used for reconstructing a 3D density map of the protein. EM single particle analyses are well suited for large soluble protein complexes and in favorable situations it is possible to reach resolutions about 4Å, like in the case of the prototypical type 1 chaperonin, GroEL (Ludtke et al., 2008). However, this methodology is not suited for proteins in an intact membrane because the membrane interaction excludes random orientations of particles.

In EM-tomography the sample is tilted step wise, collecting data from the same particle at each tilt step (usually covering ± 65˚). The advantage of this approach is that the structure of one single molecule or cellular organization can be reconstructed in 3D without averaging with other particles. Therefore, tomography has been used to determine the structure of proteins in membranes. The disadvantage with tomography is that tilting cannot cover all angels resulting in missing data. This phenomenon is known as the missing wedge and has to be correlated in the final 3D reconstruction. Another drawback is the limitation in resolution, mostly due to poor signal to noise ratio, that in the best case reaches about 25-30Å. Recently the methods of tomography and single particle analysis have been combined. This approach has especially been used to resolve the structure of the retrovirus spike in intact virus particles. EM tilt series of virus particles are collected and these are used to create a 3D model of the particle. From this subvolume of spikes are chosen and used for averaging to increase the resolution, which can reach about 18-20Å. Even if the final result do not reveal the atomic or even the secondary structure, a detailed structural map can still be obtained by fitting of parts or domains of the protein that have been solved with a high resolution method. (Frank, 2002; Roux and Taylor, 2007; Bartesaghi and Subramaniam, 2009; Spahn and Penczek, 2009).

3.8.2 CRYO-EM DATA COLLECTION.

HIV-1 spikes were isolated and samples (4 µl) applied to glow-discharged copper grids, with a thin holey carbon film mounted in a Fei Vitrobot^{TM}. After 40 s adsorption the grids were blotted once (3 seconds at zero offset) and plunge frozen in nitrogen cooled liquid ethane. All EM data was recorded in a JEOL2100F field emission gun transmission electron microscope, at 200 kV accelerating voltage and a magnification of 43,300, with a 4K x 4K CCD camera (Tiez Video and Image processing System) using 15 µm pixel size. This corresponds to 3.5 Å at the specimen level. All data were collected under low dose conditions (~10 e/Å^2) using underfocus values in the range 2.5-6 µm. The best pictures are obviously taken in perfect focus. However, cryo-EM of biological samples in focus produces little contrast making it impossible to track the particles. By taking pictures somewhat underfocused the phase contrast is increased making it possible to imagine the particles. The underfocus also leads to a systematic alteration of the image data and this alteration is described as the contrast transfer function (CTF), which needs to be corrected for each individual image during the data processing.

3.8.3 SINGLE PARTICLE DATA PROCESSING.

Image processing and 3D reconstructions were done in the EMAN package version 1.9 using standard single particle procedures (Ludtke et al., 1999). For each reconstruction about 3,000-10,000 particles, i.e. 2D images of protein complexes, were selected and visually verified in *boxer*. The particles were corrected for CTF by phase flipping using *ctfit* and used to generate an initial 3D model in *startcsym*. The initial model was refined by iterative rounds of alignment, classification and averaging until no further improvement could be achieved. In the process each round results in a new 3D model which is used to prime the following round of refinement. As the retroviral spikes were isolated as homotrimers a 3-fold symmetry was imposed throughout the reconstruction. To estimate the resolution of the final 3D reconstruction the particles were randomly split in two sets, assembled into individual 3D models and compared using a Fourier shell correlation curve (FSC) in *eotest*. The resolution was taken as the point where the FCS curve reached 0.5. The final 3D reconstructions were low pass filtered to remove information beyond the estimated resolution.

3.8.4 MOLECULAR MODELING.

In order to obtain a more detailed picture of the spike structure several different high resolution atomic models of the gp120 core protein were fitted into the EM derived 3D models (density maps) of the unliganded and CD4-bound JR-FL gp160SOSΔCT spike. To this end the gp120 core structure was extracted from (1) its complex with the b12 Fab (PDB NY7), (2) its complex with CD4 and X5 Fab (PDB 2B4C) a structure which

contain the V3 loop and (3) its complex with CD4 and 48d Fab (PDB 3JWD) which encompass the intact N- and C-terminal ends of the gp120. The fitting was done in the program *O* and was guided by overall shape similarity at a series of density thresholds. As a control the fitting was repeated using the *fit in map* utility in the program *Chimera.*

4. RESULTS AND DISCUSSIONS

4.1 KINETIC ANALYSES OF THE SURFACE-TRANSMEMBRANE DISULFIDE BOND ISOMERIZATION-CONTROLLED FUSION ACTIVATION PATHWAY IN MOLONEY MURINE LEUKEMIA VIRUS (PAPER I).

Previously it was shown that isomerization of the covalent bond between SU and TM was required for MLV membrane fusion (Wallin et al., 2004). The major evidence for this was the finding that receptor binding exposed the isomerization active thiol of the CXXC-motif of SU for modification by alkylation. This arrested the activation process of the spike at an intermediate state called the isomerization arrested stage, IAS, which could be rescued by external reduction of the intersubunit disulfide with e.g. DTT (Wallin et al., 2004). However, the direct receptor induced isomerization of the SU-TM disulfide had not been demonstrated. Further, the isomerization reaction as well as the process of thiol exposure had to be correlated with the membrane fusion reaction.

To demonstrate receptor-triggered SU-TM isomerization directly [^{35}S]-Cys labelled Mo-MLV were bound to receptor positive XC cells and to receptor negative DF-1 cells for 1h in the cold (4°C). The cultures were then incubated in fusion activation buffer for different times (0-40 min) at 37°C. During this time receptor bound Envs were triggered for isomerization and fusion activation. Thereafter, samples were lysed with NP-40 supplemented with M135. At these conditions all Envs, that had not been receptor activated were induced to isomerize but blocked by alkylation. Detergents like NP-40 and Triton X-100 are very strong inducers of SU-TM disulfide isomerization *in vitro*. Viral proteins were captured using immunoprecipitation and analyzed by SDS-PAGE at non-reducing conditions. The receptor triggered isomerization was followed by the decrease of SU-TM complexes and the increase of free SU and TM. It was found that the intersubunit disulfide isomerized with time on XC cells but not on DF-1 cells. Maximally about 30% of SU-TM isomerized. Importantly the isomerization kinetics correlated with the fusion kinetics that had been determined before. This showed that the receptor binding to Env resulted in SU-TM disulfide rearrangement and that the disulfide isomerization reaction was an integrated part of the spike activation mechanism.

We then analyzed the kinetics of formation of the alkylated, isomerization-blocked Env. [^{35}S]-Cys labelled Mo-MLV was bound to receptor positive rat XC-cells for 1h in the cold (4°C). The cultures were then incubated in fusion activation buffer containing M135 at 37°C, chasing Env to the alkylated form. After different times (0-40 min) cells were put on ice and M135 was carefully washed away. Thereafter samples were lysed in NP-40 lysis buffer, which triggers isomerization in all Envs that had not been trapped at IAS, i.e. receptor activated and blocked by alkylation during the 37°C incubation. The amount of Env at IAS was followed by immunprecipitation of the Envs and analyses of

complexed and isomerized (free) forms of the SU and TM subunits using nonreducing SDS-PAGE. We found up to 12% of Env as alkylated, isomerization arrested Env. Most significantly, the kinetics of Env alkylation followed the fusion kinetics. This suggests that the alkylated Env represented a true fusion intermediate.

The fusion kinetics observed for XC cell bound Mo-MLV should reflect the time it takes for the individual virus particles to form complete fusion sites. The receptor activation of SU-TM, in the presence of M135, generates IAS intermediates with the same kinetics as the fusion reaction. This suggests that SU-TM complexes at IAS should be assembled in arrested fusion sites. To test this possibility we analyzed the fusion kinetics after releasing the fusion activity stored in the IAS complexes. This was done by artificially reducing the intersubunit disulfide bound using DTT. According to our model we expected a rapid and synchronized release of the arrested fusion activity. Virus particles were bond to XC cells and then incubated for 15 min at 37˚C in the presence of M135. After washing M135 away, the samples were incubated for 1 to 15 min at 37˚C in the presence of DTT. The virus spikes were then inactivated by pH 3.0 treatment and the DTT-released fusion activity measured by following virus mediated cell-cell fusion. The analysis showed that already 1 min of incubation was enough for maximal fusion rescue. The fusion efficiency corresponded to about 70% of that of a nonarrested control virus. The 1 min DTT incubation was also shown to be sufficient for reducing the SU-TM disulfide of [^{35}S]-Cys labelled MLV containing receptor activated IAS spikes on XC cells. These results suggest that the SU-TM complexes of IAS intermediate spikes are located in arrested fusion sites.

In this study we also investigated how the stage of isomerization arrest related to that of hemifusion between the outer leaflets of the viral and cell membranes. For this purpose the drug chlorpromazine (CPZ) was used. CPZ lowers the energy needed for membranes to fuse. Thus, the stage of hemifusion proceeds effortlessly into complete fusion. First the effect of CPZ was investigated in our nonarrested fusion assay. To this end virus was bound to XC cells and incubated for 1 min at 37˚C with or without CPZ. This was followed by 15 min incubation at 37˚C without the drug. At this stage most viruses should have fused with the cells. Any remaining virus was inactivated by the pH 3.0 wash and cultures were incubated at 37 ˚C to reveal polykaryons of cells fused by the virus. These were used to measure viral fusion efficiency. It was observed that the sample incubated with CPZ had about 5 times more membrane fusion than the control. This showed the potency of CPZ to increase fusion, but could it rescue the membrane fusion activity of the spike at IAS? To find out, virus particles were bound to XC cells and incubated for 15 min, at 37˚C, in the presence of M135. Thereafter, cells were incubated with and without CPZ, followed by pH 3.0 inactivation and further incubation for polykaryon formation. No cell-cell fusion was detected in the sample treated with CPZ, meaning that the IAS intermediate Env does not induce hemifusion between the viral and the cell membrane. Thus the IAS intermediate has been arrested at a stage before lipid mixing.

One interesting notion in this work was the difference in amount of receptor activated Env in different assays. Maximally 12% of activated Env was detected as IAS after a 30 min incubation of virus on XC cells in the presence of M135. When isomerization was followed directly, up to 30% of the spikes were found to be activated. How can we explain this discrepancy? One explanation could be that one Env trimer binds only to one receptor. When M135 is present this will only alkylate the subunit that actually bound to the receptor whereas the other two subunits remain unactivated and will not form the IAS. In the direct isomerization assay the receptor also binds to one SU, but then activates the other two subunits in the trimer *in trans*, leading to isomerization of all three subunits. This activation model is somewhat similar to how soluble RBD can rescue the function of the ΔH8 spike mutant of Mo-MLV. An alternative explanation is that the fusion of the viral membranes with the cell membrane, that follows the direct isomerization, but not IAS formation, could potentially lead to unspecific isomerization of the SU-TM disulfide.

4.2 R-PEPTIDE CLEAVAGE POTENTIATES FUSION-CONTROLLING ISOMERIZATION OF THE INTERSUBUNIT DISULFIDE IN MOLONEY MURINE LEUKEMIA VIRUS ENV (PAPER II).

The finding in our group that MLV Env fusion is controlled by rearrangement of the covalent bond between SU and TM raised the intriguing possibility that R-peptide cleavage is needed for isomerization and the subsequent fusion activation. This possibility was investigated by creating mutations previously known to inhibit R-peptide cleavage using fusion-PCR. Substitution mutations, L649V (LV), L649I (LI), L649R (LR) and V650I (VI) were inserted into Env of the complete Mo-MLV provirus (pNCA) (Colicelli and Goff, 1988). Virus particles were produced by calcium phosphate/DNA coprecipitation-transfection into 293T cells. Virus particles were collected between 24-48 h post transfection from the cell medium. Env incorporation into particles and R-peptide cleavage were analyzed for the different mutants using [^{35}S]-Cys labelled particles. The virus was purified in a sucrose step gradient and analyzed by SDS-PAGE. The mutants and wt virus were found to be produced in similar amounts and all, but VI, contained corresponding amounts of Env. VI contained 63% of the amount of Env that was incorporated into wt virus. The LI, LV and LR mutants were significantly inhibited in R-peptide cleavage as compared to wt. In contrast, VI was cleaved as wt virus.

The fusion efficiency of the mutant viruses were tested using the virus dependent cell-cell fusion assay (fusion-from-without). The virus was bound to XC cells by centrifugation at 850 x g for 1 h at +4 °C and then incubated at 37 °C for 30 min. Under these conditions competent virus will fuse with the cells and mediate cell-cell fusion. The spikes of non-fused virus were inactivated by a low pH (pH 3.0) wash and the cells were further incubated for 3 h at 37 °C to facilitate polykaryon formation between fused cells. Polykaryons were used to calculate the fusion efficiencies of the mutants relative to that of wt. We found that the R-peptide cleavage inhibited mutants were significantly inhibited in fusion. The infectivities of the mutants were tested using a similar assay. However, after the low pH inactivation step the cells were trypsinized, seeded on coverslips and incubated for 16 h at 37 °C and screened for infection by immunoflourescense using an anti Gag monoclonal antibody. We found that the R-peptide cleavage defective mutants had significantly reduced infectivity.

To investigate if R-peptide cleavage was needed for isomerization of the SU-TM disulfide, [^{35}S]-Cys labelled mutants and wt virus were bound to target cells and then incubated for 0-30 min at 37 °C in the presence of M135. This locked the receptor triggered Envs in the IAS form. The alkylator was washed off and cells were lysed with NP-40, inducing isomerization in all unalkylated Envs. Analyses of immunoisolated Env proteins by non-reducing SDS-PAGE revealed reduced isomerization in all R-peptide cleavage deficient mutants. Additionally, we analyzed the Env isomerization capacity of the mutants by Ca^{2+}-depletion induced triggering *in vitro*. Incubation of wt

virus in buffers lacking Ca^{2+} removes an Env-stabilizing Ca^{2+}, resulting in CXXC-thiol ionization and subsequent intersubunit disulfide isomerization (Wallin et al., 2004). Accordingly, the mutants and the wt virus were taken up in TN buffer (pH 8.0) without Ca^{2+} and incubated for 0-5 h at 37 °C. NEM was added during sample lysis to prevent lysis-induced isomerization and the viral proteins immunoisolated for SDS-PAGE at non-reducing conditions. We found that the cleavage defective mutants all had a reduced isomerization kinetics compared to wt virus. However, it should be noted that all mutants were still able to complete their isomerization reaction in 5 h. The R-peptide mutants, LV and LI contained varying, small amounts of processed TM i.e. Pr15E that was cleaved into p15E. When tracking the isomerization for the SU-Pr15E and SU-p15E complexes of the mutants separately, it was apparent that it was the SU-Pr15E complexes that were inhibited in isomerization whereas the R-peptide cleaved SU-p15E complexes showed wt like isomerization.

The results showed that the R-peptide interferred with SU-TM isomerization or any preceding steps, including receptor binding. We have not been able to find proof in the literature that R-peptide containing spikes actually bind to receptors. However, the receptor independent *in vitro* Env activation assay using Ca^{2+}-depletion clearly showed that isomerization was hampered for R-peptide cleavage deficient mutants compared to wt virus. Thus, the inhibited isomerization for R-peptide cleavage deficient mutants is apparently not due to hindered receptor binding. The fact that the R-peptide cleavage deficient Env mutants were all able to completely isomerize *in vitro* during extended incubation, suggests that slow isomerization might not be the whole explanation for the almost complete fusion inhibition that was observed for the mutants. The R-peptide containing CT has previously been suggested to stabilize the Env oligomers through formation of a C-terminal coiled coil structure (Taylor and Sanders, 2003). This could prevent receptor induced changes in the Env that activate isomerization and also prevent downstream activation including TM backfolding. The R-peptide coiled-coil hypothesis has been supported by mutations in the R-peptide designed to destabilize a coiled-coil structure. Such mutants were shown to rescue fusion despite the retention of the R-peptide. To find out the most critical steps that are inhibited in the fusion activation process of the R-peptide cleavage deficient mutants, a structural approach appears necessary.

4.3 Cooperative Cleavage of the R-Peptide in the Env Trimer of the Moloney Murine Leukemia Virus Facilitates its Maturation for Fusion Competence (paper III).

The MLV spike consists of Env trimers and we wanted to investigate how the R-peptide cleavage is regulated within the trimer. Our working model proposed that when one R-peptide is cleaved this facilitates the cleavage of the other two. Thus a cooperative R-peptide cleavage within the trimer is needed for efficient fusion activation. This hypothesis was tested by using Mo-MLV particles with partially cleaved R-peptide and an R-peptide specific antibody (αR) used for immunoprecipitation of intact SU-TM (Env) trimers, i.e. spikes. First we showed that αR did not cause trimer dissociation. For this purpose spikes from the R-peptide cleavage deficient mutant LR were solubilized and incubated together with different concentrations of αR. The spike and the spike-antibody complexes were analyzed using BN-PAGE. This revealed the uncomplexed spike as SU-TM (Pr15E) trimers and the antibody-spike complexes as larger molecular associations. We concluded that the αR antibody does not dissociate the spike. To test the detection of Env heterotrimers, i.e. spikes with R-peptide cleaved (SU-p15E) and uncleaved Env (SU-Pr15E), we used a virus preparation cotransfected with wt and LR provirus DNA. We expected that wt and LR Env should form mixed trimers during biosynthesis in the ER and that the wt but not the LR TM (Pr15E) should be processed by the viral protease into p15E in the released particles. The wt/LR virus preparation was solubilized and immunoprecipitated using αR and analyzed by reducing SDS-PAGE. This showed that the αR precipitated not only SU-Pr15E, as expected, but also a significant amount of SU-p15E complexes. Thus the wt/LR virus carried spikes consisting of SU-Pr15E / SU-p15E heterotrimers.

To analyze the possibility of cooperative cleavage of Env R-peptides in the spikes of virus particles it was necessary to study a virus where the cleavage process was still incomplete. For this task we used the R-peptide cleavage deficient mutants L649I and L649V. These still supported about 10% and 20%, cleavage of Pr15E to p15E respectively. Thus, if heterotrimers were found it should be possible to coprecipitate SU-p15E with SU-Pr15E using αR. The immunoprecipitation assay did not reveal any coprecipitation of SU-p15E complexes from the lysed LV and LI mutants as found for the wt/LR virus. This suggested that R-peptide cleavage was a cooperative event within the trimer.

Further we followed R-peptide cleavage in newly assembled wt virus. This was done using MOV-3 cells producing Mo-MLV. The cells were labelled with [^{35}S]-Cys for 4 h and then virus particles were collected during 20 min. This newly released virus had about 40% of TM cleaved into p15E. By further incubating samples of the virus preparations at 37^{o}C the amount of R-peptide cleavage could be increased. Thus we had the perfect samples to investigate if cleavage of the R-peptide generated SU-Pr15E / SU-p15E heterotrimers or SU-Pr15E and SU-p15E homotrimers. The samples were

immunoprecipitated with αR and no coprecipitation of SU-p15E with SU-Pr15E complexes was detected. This supported our model of cooperative R-peptide cleavage generating preferentially SU-p15E homotrimers rather than SU-Pr15E / SU-p15E heterotrimers. Next we wanted to investigate if the cooperative R-peptide cleavage was important for activation of the membrane fusion function of the spike. This was done by comparing two virus preparations with equal, about 50%, cleavage of the R-peptide, but where one contained heterotrimers and the other one homotrimeric spikes. The wt/LR virus represented the sample with heterotrimeric spikes and the sample with homotrimeric spikes was wt virus prepared in the presence of the virus protease inhibitor amprenavir. The drug preferentially inhibits the R-peptide cleavage over Gag cleavage. The virus dependent cell-cell fusion assay (fusion-from-without) showed that the wt/LR virus was significantly reduced in cell-cell fusion compared to the wt/amprenavir virus. Thus, the cooperative R-peptide cleavage facilitated the maturation of the viral spike for fusion competence. Our results about the cooperative cleavage of the R-peptides in one spike are consistent with previous data suggesting that the endodomains of SU-Pr15E trimers form a stable coiled-coil structure that suppresses the activation of the spike (Taylor and Sanders, 2003). In such a structure the cleavage of the R-peptide in one TM subunit is expected to disrupt the coiled-coil interaction, possibly resulting in the release of the uncleaved R-peptide tails of the other two subunits in a protease sensitive form.

Surprisingly, when wt/LV and wt/LI virus were prepared by cotransfection of 293T cells with corresponding proviral DNAs, we found that they contained mostly R-peptide cleaved Env in their spikes and that SU-p15E, and the minor amount of SU-Pr15E complexes left, were forming homotrimers. This suggested that the mutated cleavage sites of the LV and LI SU-Pr15E complexes were cleaved in heterotrimers formed with the wt SU-Pr15E complexes. To make sure that this apparent cleavage rescue was not due to selective wt Env incorporation into virus an Influenza HA epitope was inserted into the PRR region of the LI and LR spike mutants using fusion-PCR. Previously, it was shown that the PRR tolerated insertion of the HA epitope and that this was exposed for antibody binding (Ou et al., 2006). The mutants created were referred to as LI-HA and LR-HA. Wt/LI-HA and wt/LR-HA viruses were then prepared by proviral DNA transfection of 293T cells and the viral spikes analyzed by αHA immunorecipitation. It was expected that upon cleavage-rescue in wt/LI-HA virus that αHA should precipitate relatively more SU-p15E complexes from wt/LI-HA virus than from wt/LR-HA virus, where no cleavage-rescue of mutated Env occurs. If LI-HA spikes were blocked in virus incorporation, no immunoprecipitable complexes should be formed in the wt/LI-HA virus. The result showed that SU-TM complexes were efficiently precipitated and that much more SU-p15E complexes were precipitated from lysed wt/LI-HA virus than from wt/LR-HA virus. This proved the rescue of the R-peptide cleavage of LI-HA in wt/LI-HA heterotrimers and further supported the R-peptide cooperative cleavage mechanism. Accordingly, the cleavage of the CT in the wt SU-Pr15E complexes of wt/LI SU-Pr15E heterotrimers, possibly with their CTs as a coiled-coil, will present the CT of the mutant

SU-Pr15E complexes in a form that is cleaved by the viral protease. Notably, the mutant SU-Pr15E complexes are almost completely cleavage-inhibited when present in homotrimers, probably because cleavage of the first R-peptide in a trimer is difficult. The rescue results show that the original rule, that amino acids branched at the β-carbon are not tolerated at the P1 position of the cleavage site, does not hold at the condition of a wt/mutant SU-Pr15E heterotrimer. However, charged cleavage site changes at this position, like in the LR mutant, cannot be cleaved even if the mutant SU-Pr15E complex is present in heterotrimers with wt complexes.

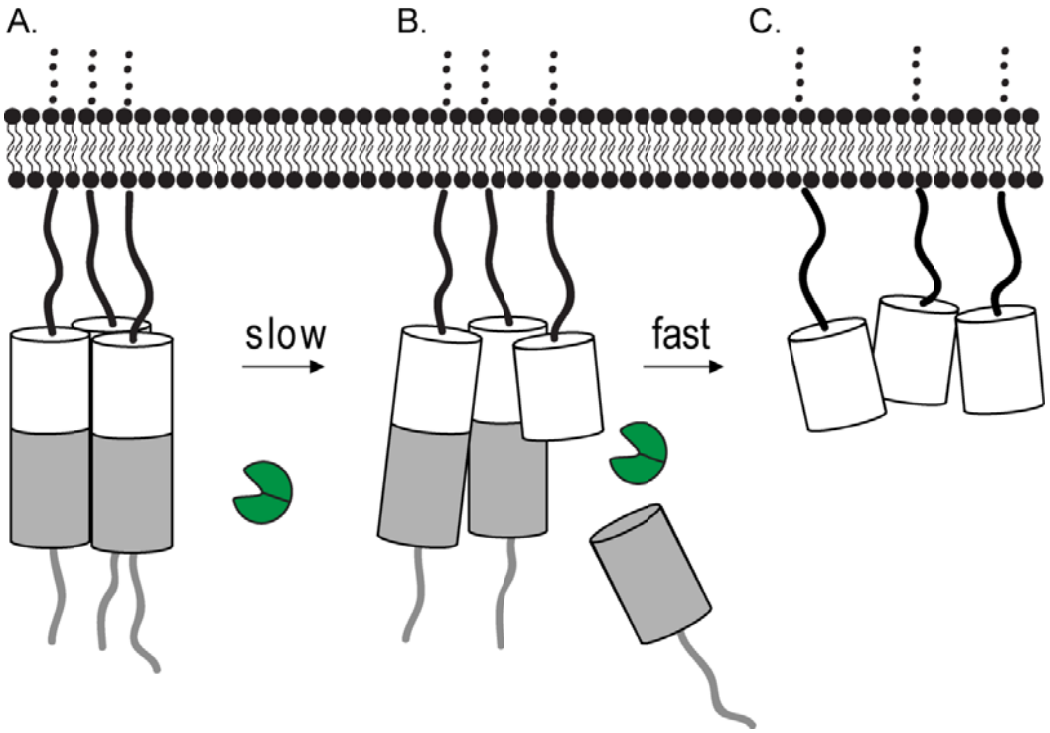

Fig 16. A molecular model for cooperative R-peptide cleavage. The putative coiled coil structure in the cytoplasmic tail of the MLV spike is illustrated as three barrels. The grey color represent the R-peptide and the white color the residues involved in coiled coil formation that are located upstream of the R-peptide cleavage site. The viral protease is shown in green. (A) The PR cleavage site is sterically hidden in the coiled coil resulting in slow R-peptide cleavage. (B-C) When one R-peptide is processed this disrupts the coiled coil structure exposing the other two sites for rapid cleavage.

The cooperativity found for the R-peptide cleavage reaction in the Env trimer helps explaining how symmetry and functionality can be maintained during this structural transition. It can be speculated that cooperative cleavage within the Env trimers could be a general event in virus maturation. For example, this could be the case during the furin cleavage of Env trimers into their separate SU and TM subunits. It is also possible that cooperative protease cleavage applies to the processing of Gag into its separate proteins, especially when this event is known to be executed quickly during the time limit of viral budding.

4.4 Single-Particle Cryoelectron Microscopy Analysis Reveals the HIV-1 Spike as a Tripod Structure (paper IV).

The 3D structure of the native HIV-1 spike has so far only been determined using cryo-EM tomography with applied single particle technique. The resulting structures, from different groups, have been very dissimilar. These showed either a hollow spike head, which was connected to the viral membrane by a stem or a more compact spike with three feet. We wanted to use the well established methodology of single particle cryo-EM and 3D reconstruction using the software EMAN to determine the structure of the native and CD4 receptor activated HIV-1 spike, i.e. the gp trimer. Our aim was to understand the initial conformational changes in the gp trimer during HIV-1 fusion activation. Due to gp120 shedding from virus particles incubated with soluble CD4 (sCD4) we decided to work with a modified gp construct where the gp120 and gp41 subunits were covalently linked by a disulfide. The modifications involved the introduction of a Cys into the C5 domain of gp120 and another Cys downstream of the disulfide loop region ($CX_5C \rightarrow CX_5CC$) of gp41 (Binley et al., 2000). This gp, gp160SOS, has been shown to assemble into HIV-1 particles that upon CD4 receptor and coreceptor binding are trapped in an intermediate state of fusion activation. Treatment of the intermediate with a reducing agent (DTT) reduced the introduced disulfide bond and rescued membrane fusion (Abrahamyan et al., 2003; Binley et al., 2003). Thus binding of sCD4 to gp160SOS should trigger the initial conformational changes without causing gp120 shedding. To increase the amount of Env incorporation into particles the cytoplasmic tail of TM was also deleted. The resulting gp was called gp160SOSΔCT (Binley et al., 2000). Virus particles containing gp160SOSΔCT were produced in 293T cells transfected with the DNAs encoding the modified gp and the proteins for particle formation. Virus particles were soloubilized with Triton X-100 and gp trimers were purified using sucrose gradient centrifugations. The gp trimers, or sCD4 bound gp trimers, were then applied to holey carbon grids and immediately plunged frozen. EM pictures were taken using a JEOL2100F field emission transmission electron microscope with an accelerating voltage of 200 kV. Gp trimers were selected from the micrographs and used for reconstruction of their 3D structures.

We found that the native HIV-1 gp trimer formed a hollow cage-like structure with 3-fold interaction at the top and at the bottom. The gp protomeric unit could be divided into a common roof, a lobe and a leg on the side of the cage and a bottom part. The gp120 core atomic structure obtained in complex with the b12 Fab (Zhou et al., 2007) is believed to represent a close to native conformation and this structure fitted into our lobe density in a unique orientation. The CD4 binding site was located to the outer surface of the lobe and the silent face known to be extensively glycosylated was exposed to the surface. The stems of the deleted V1-V2 and V3 loops pointed into the roof suggesting these loops to occupy this region and to be responsible for the trimer interactions. We also fitted the atomic gp120 core structure with intact N- and C-terminal ends obtained in complex with CD4 and 48d Fab (Pancera et al., 2010). The

30Å long N/C extension followed the density of the entire length of the leg in our 3D structure, validating its tripod nature.

The hollow cage like structure was also clearly recognized in the CD4 bound HIV-1 spike structure. However, three new protrusions appeared in the roof about 30Å from the center of the 3-fold axis. There was also a new protrusion in the upper part of the lobe. In general the CD4 binding caused a shift of density from the center of the roof to the periphery. In the bottom part of the liganded spike there was a shift of density from the peripheral bodies in the native structure to a central body instead. The CD4 bound atomic gp120 core structure with intact N- and C-terminals fitted perfectly into the lobe and leg densities. The atomic structure of the CD4 bound gp120 core containing an intact V3 loop also fitted into our density map of the CD4 bound spike. The V3 loop occupied the roof protrusion, the stem of the V1-V2 loops pointed into the lobe protrusion, whereas the core structure had almost the same fit in the lobe as in the native spike. This suggested that CD4 binding did not change the position of the gp120 core, but caused major conformational changes i.e. V3 was lifted up and V1-V2 displaced laterally. Similar displacement of the V1-V2 and V3 regions were previously described by Liu et al. in their cryo-EM tomography study, when they compared the structural transition between the native HIV spike and the CD4 activated spike stabilized by 17b Fab binding. However in their case, the structural transition was explained by a significant gp120 rotation.

We believe that the V1-V2 loops cover the V3 loop and together they make the three fold interactions in the roof region in the native spike. This has been suggested before by epitope mapping and by the demonstration of a functional interplay between the V1-V2 and V3 loops (Thali et al., 1993; Wyatt et al., 1995; Sullivan et al., 1998). It has also been shown that the V3 loop has conserved structural elements that could be important for these interactions (Jiang et al., 2010). In further support for our loop interaction model, there were recently two different cryo-EM tomography studies of SIV and HIV containing V1-V2 deletions. In general they confirmed a hollow spike head structure, but in both cases it was noted that the deletions resulted in loss of density at the three fold axis in the roof of the hollow spike (White et al., 2010; Hu et al., 2011). Our present results suggest that CD4 binding causes lateral displacement of the V1-V2 loops and the raising up of the V3 loops, apparently for coreceptor binding. This is supported by earlier biochemical studies (Wyatt et al., 1995; Sanders et al., 2000).

The organization of gp41 in our spike structure remains elusive. The crystal structure of the post fusion gp41 does not fit into our unliganded or liganded spike density (Weissenhorn et al., 1997). This suggests that gp41 is not, as expected, arranged as a six helical bundle in either the native or the CD4 liganded spike. The C-terminal residue (A501) of the gp120 core structure containing the N/C-extension is in the gp160SOSΔCT construct substituted with the Cys that makes the covalent bond with the disulfide loop region of gp41. Thus, the latter part of gp41 should be located in the lower part of the leg in our spike density map. From here it is possible that the N-

terminal region of the gp41 ectodomain, containing the N-helix and fusion peptide, ascends along the N/C extension until the inner domain β- sandwich. This is supported by the findings that mutations in the N/C extension and inner domain β-sandwich lead to dissociation of gp120 and gp41 (Finzi et al., 2010). The C-terminal part of gp41 containing the C-helix and the MPER could together with the transmembrane region compose the peripheral body of the spike bottom.

Our native spike structure is similar to that of Liu et al in the head region. Both contain a cavity with a roof and side lobes where the gp120 core structure fits. The dissimilarities between the two structures are mainly observed in the lower part of the molecule. Liu et al, reported a compact gp41 stalk, while we have an obvious tripod leg structure. However, the gp120 core structure containing the N/C extension pointed out of the density in the structure published by Liu et al. Thus the stem structure remains unvalidated. To explain this inconsistency it was suggested that the N/C extension was flexible and that the crystal structure might resemble an intermediate structure important for fusion (Pancera et al., 2010). However, the gp120 core structure with N/C extension fits perfectly into our spike density. The validity of our spike structure was further corroborated by several control reconstructions designed to exclude solubilization and cross-linking artifacts. In addition, the tripod structure we observed finds support from earlier cryo-ET studies of SIV and MLV (Forster et al., 2005; Zhu et al., 2006).

There are several apparent similarities between the structure and function of the HIV-1 and Mo-MLV spikes. The outer domain of the HIV-1 gp120 core with the V3 loop has similar functions as the MLV RBD. They are both heavily glycosylated, binds to the host cell receptor (mCAT-1 and the chemokine receptor) and are believed to transmit a signal to the rest of the fusion complex upon activation. The HIV-1 bridging sheet and the MLV PRR are also having functional similarities. They are both described as flexible regions transmitting a signal from the receptor binding domain to a region of the peripheral subunit interacting with the transmembrane subunit, i.e. the inner domain of the HIV-1 gp120 core and the Mo-MLV CTD, respectively. Further, the HIV-1 inner domain together with the N/C-extension is thought to interact with gp41. Upon activation this interaction is changed, releasing gp120 from gp41 and activating the metastable gp41. This function is similar to that of the MLV CTD. Here receptor binding transmits a signal, resulting in isomerization of the disulfide between SU and TM, leading to activation of TM for membrane fusion. Considering these functional similarities it is not surprising that the HIV-1 spike structure reported here has several similarities compared to the previously published MLV spike structure. They both share the hollow cage like feature with a compact roof, legs and lobes on the side of the cavity and a bottom part with peripheral bodies. The biggest difference between the two structures is the large middle protrusion in MLV. This protrusion might contain the disulfide isomerase region of MLV SU. Thus, not surprising, it is not present in the HIV-1 spike. In addition, the initial conformational changes observed upon fusion activation in the IAS form for MLV and in the CD4 bound spike for HIV-1 result in the

opening of the cage roof. This most likely represents the first structural transition that eventually leads to the dissociation of the gp120-gp41 and SU-TM complexes and fusion. A synchronized opening of the roof could guide and make space for a gp41 (or TM) prehairpin to reach the cell membrane with its fusion peptide.

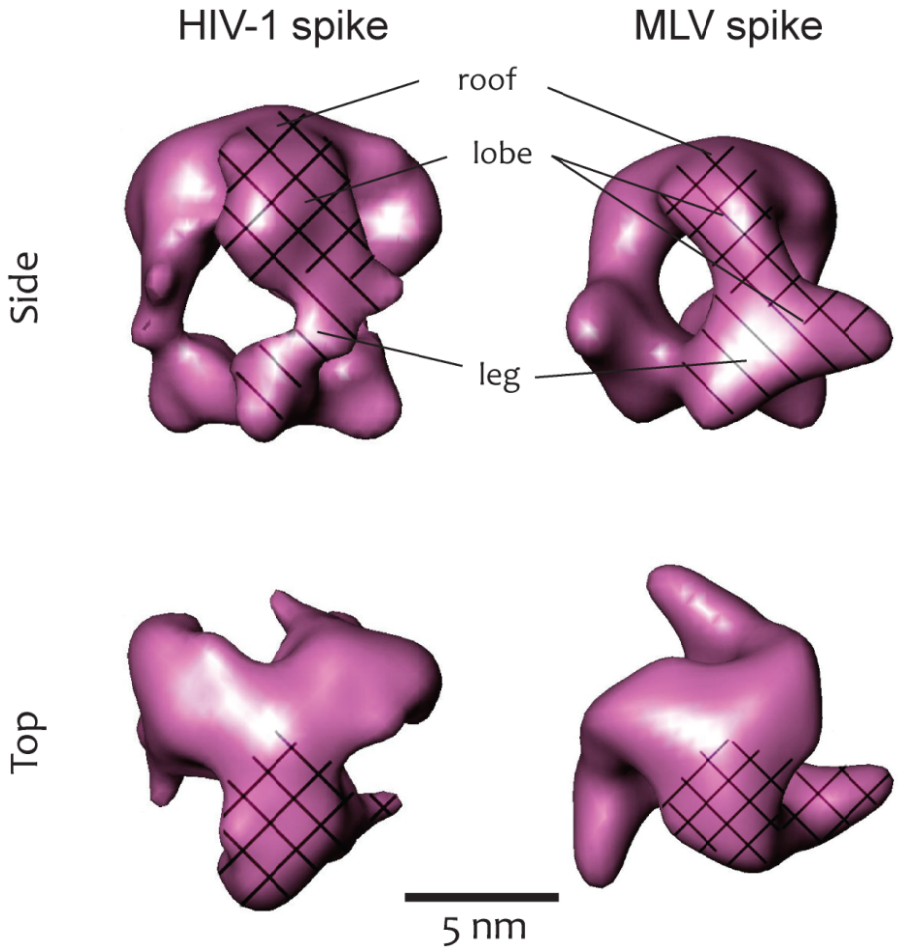

Fig 17. Comparison between HIV-1 and Mo-MLV spike structures determined using Cryo-EM single particle analysis. Both the HIV-1 spike (left, 18Å resolution) and the Mo-MLV spike (right, 19Å resolution) have the same general structure. They share the hollow cage like feature, the compact roof, legs and lobes on the side of the cavities and a bottom part with three peripheral bodies.

5. ACKNOWLEDGEMENTS

The work in this thesis was carried out at the Karolinska Institute, Department of Biosciences and Nutrition.

First I would like to thank my supervisor **Henrik Garoff** for all thorough discussions and for always giving me the freedom to decide what project or experiment to work on. This has not always been the most time efficient strategy in the hunt for publications, but absolutely the best strategy to teach the concept of science.

Mathilda Sjöberg, thank you for all discussions and suggestions, this has improved my laboratory skills and the quality of my publications. Hopefully the best paper is still to come! I would also like to thank you for revising this thesis.

Rickard Nordström, thank you for sharing your brilliant mind and always answering my questions with plenty of facts. You have really increased my biochemical and computer skills, hopefully this combination can lead to other achievements.

Sunny Wu, thank you for always helping me when I struggle with EMAN, the HIV-1 project could not have been done without you. I hope all your future plans come true! I would also like to thank you for the assistance in making some of the pictures in this thesis.

Michael Wallin, thank you for all help during my exam work and for all good ideas and suggestion. I will not forget "The Supperhaar" and "The Amazing Spray Tan". I wish you all the best in the future!

Birgitta Lindqvist, thank you for keeping me alert and always prepared for an assault! Your laboratory skills are truly amazing; sadly your "coconut-tasting-cocktail" drinking skill do not match up!

Kejun Li and **Shujing Zhang**, thank you for your support and helpful advice.

Kimmo Rantalainen, even though you have a “bomfunk MC” origin, you are a great guy! I am looking forward to some “salsi” and hopefully we will be able to accomplish some of our plans.

Maria Ekström and **Malin Kronqvist**, thank you for assistance and for making sure I fulfill my cake club obligations.

Lars Haag, thank you for believing in me and Rickard, you are a true puppet master! Maybe this summer we can realize our fishing plans.

Krishan Johansson Hague, thank you for challenging me in arm wrestling, giving me the opportunity to prove my superior physical strange! It is pleasant to have you around and keep up the good work.

Anna Ingemarsdotter and **Mimmi Kotka** you are both excellent although your healthy life styles are not that well synced with me. Maybe we can plan lunch in the “bunker” this summer? Anna I truly wish you and your white iPhone 4 all happiness in the future!

Finally I would like to thank the love of my life, **Nakisa** and our daughter **Leana**. Thank you for all support and understanding, now we will have more time together!

6. REFERENCES

Abrahamyan, L.G., Markosyan, R.M., Moore, J.P., Cohen, F.S., and Melikyan, G.B. (2003). Human immunodeficiency virus type 1 Env with an intersubunit disulfide bond engages coreceptors but requires bond reduction after engagement to induce fusion. Journal of virology 77, 5829-5836.

Aguilar, H.C., Anderson, W.F., and Cannon, P.M. (2003). Cytoplasmic tail of Moloney murine leukemia virus envelope protein influences the conformation of the extracellular domain: implications for mechanism of action of the R Peptide. Journal of virology 77, 1281-1291.

Alam, S.M., Morelli, M., Dennison, S.M., Liao, H.X., Zhang, R., Xia, S.M., Rits-Volloch, S., Sun, L., Harrison, S.C., Haynes, B.F., and Chen, B. (2009). Role of HIV membrane in neutralization by two broadly neutralizing antibodies. Proceedings of the National Academy of Sciences of the United States of America 106, 20234-20239.

Albritton, L.M., Tseng, L., Scadden, D., and Cunningham, J.M. (1989). A putative murine ecotropic retrovirus receptor gene encodes a multiple membrane-spanning protein and confers susceptibility to virus infection. Cell 57, 659-666.

Aloia, A.L., Sfanos, K.S., Isaacs, W.B., Zheng, Q., Maldarelli, F., De Marzo, A.M., and Rein, A. (2010). XMRV: a new virus in prostate cancer? Cancer research 70, 10028-10033.

Bae, Y., Kingsman, S.M., and Kingsman, A.J. (1997). Functional dissection of the Moloney murine leukemia virus envelope protein gp70. Journal of virology 71, 2092-2099.

Barnett, A.L., and Cunningham, J.M. (2001). Receptor binding transforms the surface subunit of the mammalian C-type retrovirus envelope protein from an inhibitor to an activator of fusion. Journal of virology 75, 9096-9105.

Barnett, A.L., Davey, R.A., and Cunningham, J.M. (2001). Modular organization of the Friend murine leukemia virus envelope protein underlies the mechanism of infection. Proceedings of the National Academy of Sciences of the United States of America 98, 4113-4118.

Bartesaghi, A., and Subramaniam, S. (2009). Membrane protein structure determination using cryo-electron tomography and 3D image averaging. Current opinion in structural biology 19, 402-407.

Bieniasz, P.D. (2009). The cell biology of HIV-1 virion genesis. Cell host & microbe 5, 550-558.

Binley, J.M., Cayanan, C.S., Wiley, C., Schulke, N., Olson, W.C., and Burton, D.R. (2003). Redox-triggered infection by disulfide-shackled human immunodeficiency virus type 1 pseudovirions. Journal of virology 77, 5678-5684.

Binley, J.M., Sanders, R.W., Clas, B., Schuelke, N., Master, A., Guo, Y., Kajumo, F., Anselma, D.J., Maddon, P.J., Olson, W.C., and Moore, J.P. (2000). A recombinant human immunodeficiency virus type 1 envelope glycoprotein complex stabilized by an intermolecular disulfide bond between the gp120 and gp41 subunits is an antigenic mimic of the trimeric virion-associated structure. Journal of virology 74, 627-643.

Blot, G., Janvier, K., Le Panse, S., Benarous, R., and Berlioz-Torrent, C. (2003). Targeting of the human immunodeficiency virus type 1 envelope to the trans-Golgi network through binding to TIP47 is required for env incorporation into virions and infectivity. Journal of virology 77, 6931-6945.

Bobkova, M., Stitz, J., Engelstadter, M., Cichutek, K., and Buchholz, C.J. (2002). Identification of R-peptides in envelope proteins of C-type retroviruses. The Journal of general virology 83, 2241-2246.

Bosch, M.L., Earl, P.L., Fargnoli, K., Picciafuoco, S., Giombini, F., Wong-Staal, F., and Franchini, G. (1989). Identification of the fusion peptide of primate immunodeficiency viruses. Science (New York, N.Y 244, 694-697.

Brody, B.A., Rhee, S.S., and Hunter, E. (1994). Postassembly cleavage of a retroviral glycoprotein cytoplasmic domain removes a necessary incorporation signal and activates fusion activity. Journal of virology 68, 4620-4627.

Carr, C.M., and Kim, P.S. (1993). A spring-loaded mechanism for the conformational change of influenza hemagglutinin. Cell 73, 823-832.

Chan, D.C., Chutkowski, C.T., and Kim, P.S. (1998). Evidence that a prominent cavity in the coiled coil of HIV type 1 gp41 is an attractive drug target. Proceedings of the National Academy of Sciences of the United States of America 95, 15613-15617.

Chan, D.C., Fass, D., Berger, J.M., and Kim, P.S. (1997). Core structure of gp41 from the HIV envelope glycoprotein. Cell 89, 263-273.

Chandran, K., Sullivan, N.J., Felbor, U., Whelan, S.P., and Cunningham, J.M. (2005). Endosomal proteolysis of the Ebola virus glycoprotein is necessary for infection. Science (New York, N.Y 308, 1643-1645.

Chatis, P.A., Holland, C.A., Hartley, J.W., Rowe, W.P., and Hopkins, N. (1983). Role for the 3' end of the genome in determining disease specificity of Friend and Moloney murine leukemia viruses. Proceedings of the National Academy of Sciences of the United States of America 80, 4408-4411.

Chen, L., Kwon, Y.D., Zhou, T., Wu, X., O'Dell, S., Cavacini, L., Hessell, A.J., Pancera, M., Tang, M., Xu, L., Yang, Z.Y., Zhang, M.Y., Arthos, J., Burton, D.R., Dimitrov, D.S., Nabel, G.J., Posner, M.R., Sodroski, J., Wyatt, R., Mascola, J.R., and Kwong, P.D. (2009). Structural basis of immune evasion at the site of CD4 attachment on HIV-1 gp120. Science (New York, N.Y 326, 1123-1127.

Chernomordik, L.V., and Kozlov, M.M. (2003). Protein-lipid interplay in fusion and fission of biological membranes. Annual review of biochemistry 72, 175-207.

Chernomordik, L.V., and Kozlov, M.M. (2008). Mechanics of membrane fusion. Nature structural & molecular biology 15, 675-683.

Coffin, J.M., Hughes, S.H., and Varmus, H.E. (1997). The Interactions of Retroviruses and their Hosts.

Colicelli, J., and Goff, S.P. (1988). Sequence and spacing requirements of a retrovirus integration site. Journal of molecular biology 199, 47-59.

Davey, R.A., Zuo, Y., and Cunningham, J.M. (1999). Identification of a receptor-binding pocket on the envelope protein of friend murine leukemia virus. Journal of virology 73, 3758-3763.

Davey, R.A., Hamson, C.A., Healey, J.J., and Cunningham, J.M. (1997). In vitro binding of purified murine ecotropic retrovirus envelope surface protein to its receptor, MCAT-1. Journal of virology 71, 8096-8102.

de Parseval, A., Chatterji, U., Sun, P., and Elder, J.H. (2004). Feline immunodeficiency virus targets activated CD4+ T cells by using CD134 as a binding receptor. Proceedings of the National Academy of Sciences of the United States of America 101, 13044-13049.

Delos, S.E., La, B., Gilmartin, A., and White, J.M. (2010). Studies of the "chain reversal regions" of the avian sarcoma/leukosis virus (ASLV) and ebolavirus fusion proteins: analogous residues are important, and a His residue unique to EnvA affects the pH dependence of ASLV entry. Journal of virology 84, 5687-5694.

Deng, H., Liu, R., Ellmeier, W., Choe, S., Unutmaz, D., Burkhart, M., Di Marzio, P., Marmon, S., Sutton, R.E., Hill, C.M., Davis, C.B., Peiper, S.C., Schall, T.J., Littman, D.R., and Landau, N.R. (1996). Identification of a major co-receptor for primary isolates of HIV-1. Nature 381, 661-666.

Dimitrov, A.S., Jacobs, A., Finnegan, C.M., Stiegler, G., Katinger, H., and Blumenthal, R. (2007). Exposure of the membrane-proximal external region of HIV-1 gp41 in the course of HIV-1 envelope glycoprotein-mediated fusion. Biochemistry 46, 1398-1401.

Doitsh, G., Cavrois, M., Lassen, K.G., Zepeda, O., Yang, Z., Santiago, M.L., Hebbeler, A.M., and Greene, W.C. (2010). Abortive HIV infection mediates CD4 T cell depletion and inflammation in human lymphoid tissue. Cell 143, 789-801.

Edwards, T.G., Wyss, S., Reeves, J.D., Zolla-Pazner, S., Hoxie, J.A., Doms, R.W., and Baribaud, F. (2002). Truncation of the cytoplasmic domain induces exposure of conserved regions in the ectodomain of human immunodeficiency virus type 1 envelope protein. Journal of virology 76, 2683-2691.

Evans, L.H., and Morrey, J.D. (1987). Tissue-specific replication of Friend and Moloney murine leukemia viruses in infected mice. Journal of virology 61, 1350-1357.

Fass, D., Harrison, S.C., and Kim, P.S. (1996). Retrovirus envelope domain at 1.7 angstrom resolution. Nature structural biology 3, 465-469.

Feher, A., Boross, P., Sperka, T., Miklossy, G., Kadas, J., Bagossi, P., Oroszlan, S., Weber, I.T., and Tozser, J. (2006). Characterization of the murine leukemia virus protease and its comparison with the human immunodeficiency virus type 1 protease. The Journal of general virology 87, 1321-1330.

Feng, Y., Broder, C.C., Kennedy, P.E., and Berger, E.A. (1996). HIV-1 entry cofactor: functional cDNA cloning of a seven-transmembrane, G protein-coupled receptor. Science (New York, N.Y 272, 872-877.

Finzi, A., Xiang, S.H., Pacheco, B., Wang, L., Haight, J., Kassa, A., Danek, B., Pancera, M., Kwong, P.D., and Sodroski, J. (2010). Topological layers in the HIV-1 gp120 inner domain regulate gp41 interaction and CD4-triggered conformational transitions. Molecular cell 37, 656-667.

Forster, F., Medalia, O., Zauberman, N., Baumeister, W., and Fass, D. (2005). Retrovirus envelope protein complex structure in situ studied by cryo-electron tomography. Proceedings of the National Academy of Sciences of the United States of America 102, 4729-4734.

Frank, J. (2002). Single-particle imaging of macromolecules by cryo-electron microscopy. Annual review of biophysics and biomolecular structure 31, 303-319.

Freed, E.O., Delwart, E.L., Buchschacher, G.L., Jr., and Panganiban, A.T. (1992). A mutation in the human immunodeficiency virus type 1 transmembrane

glycoprotein gp41 dominantly interferes with fusion and infectivity. Proceedings of the National Academy of Sciences of the United States of America 89, 70-74.
Furuta, R.A., Wild, C.T., Weng, Y., and Weiss, C.D. (1998). Capture of an early fusion-active conformation of HIV-1 gp41. Nature structural biology 5, 276-279.
Green, N., Shinnick, T.M., Witte, O., Ponticelli, A., Sutcliffe, J.G., and Lerner, R.A. (1981). Sequence-specific antibodies show that maturation of Moloney leukemia virus envelope polyprotein involves removal of a COOH-terminal peptide. Proceedings of the National Academy of Sciences of the United States of America 78, 6023-6027.
Groom, H.C., Boucherit, V.C., Makinson, K., Randal, E., Baptista, S., Hagan, S., Gow, J.W., Mattes, F.M., Breuer, J., Kerr, J.R., Stoye, J.P., and Bishop, K.N. (2010). Absence of xenotropic murine leukaemia virus-related virus in UK patients with chronic fatigue syndrome. Retrovirology 7, 10.
Hallenberger, S., Bosch, V., Angliker, H., Shaw, E., Klenk, H.D., and Garten, W. (1992). Inhibition of furin-mediated cleavage activation of HIV-1 glycoprotein gp160. Nature 360, 358-361.
Harrison, S.C. (2008). Viral membrane fusion. Nature structural & molecular biology 15, 690-698.
Henderson, L.E., Sowder, R., Copeland, T.D., Smythers, G., and Oroszlan, S. (1984). Quantitative separation of murine leukemia virus proteins by reversed-phase high-pressure liquid chromatography reveals newly described gag and env cleavage products. Journal of virology 52, 492-500.
Hohn, O., Krause, H., Barbarotto, P., Niederstadt, L., Beimforde, N., Denner, J., Miller, K., Kurth, R., and Bannert, N. (2009). Lack of evidence for xenotropic murine leukemia virus-related virus(XMRV) in German prostate cancer patients. Retrovirology 6, 92.
Hu, G., Liu, J., Taylor, K.A., and Roux, K.H. (2011). Structural Comparison of HIV-1 Envelope Spikes with and without the V1/V2 Loop. Journal of virology.
Huang, C.C., Tang, M., Zhang, M.Y., Majeed, S., Montabana, E., Stanfield, R.L., Dimitrov, D.S., Korber, B., Sodroski, J., Wilson, I.A., Wyatt, R., and Kwong, P.D. (2005). Structure of a V3-containing HIV-1 gp120 core. Science (New York, N.Y 310, 1025-1028.
Hue, S., Gray, E.R., Gall, A., Katzourakis, A., Tan, C.P., Houldcroft, C.J., McLaren, S., Pillay, D., Futreal, A., Garson, J.A., Pybus, O.G., Kellam, P., and Towers, G.J. (2010). Disease-associated XMRV sequences are consistent with laboratory contamination. Retrovirology 7, 111.
Hunter, E. (1997). Viral Entry and Receptors.
Jiang, S., Lin, K., Strick, N., and Neurath, A.R. (1993). HIV-1 inhibition by a peptide. Nature 365, 113.
Jiang, X., Burke, V., Totrov, M., Williams, C., Cardozo, T., Gorny, M.K., Zolla-Pazner, S., and Kong, X.P. (2010). Conserved structural elements in the V3 crown of HIV-1 gp120. Nature structural & molecular biology 17, 955-961.
Karlsson Hedestam, G.B., Fouchier, R.A., Phogat, S., Burton, D.R., Sodroski, J., and Wyatt, R.T. (2008). The challenges of eliciting neutralizing antibodies to HIV-1 and to influenza virus. Nature reviews 6, 143-155.
Kielian, M., and Rey, F.A. (2006). Virus membrane-fusion proteins: more than one way to make a hairpin. Nature reviews 4, 67-76.
Kirchhoff, F. (2010). Immune evasion and counteraction of restriction factors by HIV-1 and other primate lentiviruses. Cell host & microbe 8, 55-67.

Kozak, C.A. (2010). The mouse "xenotropic" gammaretroviruses and their XPR1 receptor. Retrovirology 7, 101.

Kozlov, M.M., McMahon, H.T., and Chernomordik, L.V. (2010). Protein-driven membrane stresses in fusion and fission. Trends in biochemical sciences 35, 699-706.

Kwong, P.D., Wyatt, R., Robinson, J., Sweet, R.W., Sodroski, J., and Hendrickson, W.A. (1998). Structure of an HIV gp120 envelope glycoprotein in complex with the CD4 receptor and a neutralizing human antibody. Nature 393, 648-659.

Lavillette, D., Ruggieri, A., Russell, S.J., and Cosset, F.L. (2000). Activation of a cell entry pathway common to type C mammalian retroviruses by soluble envelope fragments. Journal of virology 74, 295-304.

Lavillette, D., Boson, B., Russell, S.J., and Cosset, F.L. (2001). Activation of membrane fusion by murine leukemia viruses is controlled in cis or in trans by interactions between the receptor-binding domain and a conserved disulfide loop of the carboxy terminus of the surface glycoprotein. Journal of virology 75, 3685-3695.

Lavillette, D., Ruggieri, A., Boson, B., Maurice, M., and Cosset, F.L. (2002). Relationship between SU subdomains that regulate the receptor-mediated transition from the native (fusion-inhibited) to the fusion-active conformation of the murine leukemia virus glycoprotein. Journal of virology 76, 9673-9685.

Lavillette, D., Maurice, M., Roche, C., Russell, S.J., Sitbon, M., and Cosset, F.L. (1998). A proline-rich motif downstream of the receptor binding domain modulates conformation and fusogenicity of murine retroviral envelopes. Journal of virology 72, 9955-9965.

Li, K., Zhang, S., Kronqvist, M., Ekstrom, M., Wallin, M., and Garoff, H. (2007). The conserved His8 of the Moloney murine leukemia virus Env SU subunit directs the activity of the SU-TM disulphide bond isomerase. Virology 361, 149-160.

Li, K., Zhang, S., Kronqvist, M., Wallin, M., Ekstrom, M., Derse, D., and Garoff, H. (2008). Intersubunit disulfide isomerization controls membrane fusion of human T-cell leukemia virus Env. Journal of virology 82, 7135-7143.

Liu, J., Bartesaghi, A., Borgnia, M.J., Sapiro, G., and Subramaniam, S. (2008). Molecular architecture of native HIV-1 gp120 trimers. Nature 455, 109-113.

Lo, S.C., Pripuzova, N., Li, B., Komaroff, A.L., Hung, G.C., Wang, R., and Alter, H.J. (2010). Detection of MLV-related virus gene sequences in blood of patients with chronic fatigue syndrome and healthy blood donors. Proceedings of the National Academy of Sciences of the United States of America 107, 15874-15879.

Lombardi, V.C., Ruscetti, F.W., Das Gupta, J., Pfost, M.A., Hagen, K.S., Peterson, D.L., Ruscetti, S.K., Bagni, R.K., Petrow-Sadowski, C., Gold, B., Dean, M., Silverman, R.H., and Mikovits, J.A. (2009). Detection of an infectious retrovirus, XMRV, in blood cells of patients with chronic fatigue syndrome. Science (New York, N.Y 326, 585-589.

Lopez-Verges, S., Camus, G., Blot, G., Beauvoir, R., Benarous, R., and Berlioz-Torrent, C. (2006). Tail-interacting protein TIP47 is a connector between Gag and Env and is required for Env incorporation into HIV-1 virions. Proceedings of the National Academy of Sciences of the United States of America 103, 14947-14952.

Ludtke, S.J., Baldwin, P.R., and Chiu, W. (1999). EMAN: semiautomated software for high-resolution single-particle reconstructions. Journal of structural biology 128, 82-97.

Ludtke, S.J., Baker, M.L., Chen, D.H., Song, J.L., Chuang, D.T., and Chiu, W. (2008). De novo backbone trace of GroEL from single particle electron cryomicroscopy. Structure 16, 441-448.

Maerz, A.L., Center, R.J., Kemp, B.E., Kobe, B., and Poumbourios, P. (2000). Functional implications of the human T-lymphotropic virus type 1 transmembrane glycoprotein helical hairpin structure. Journal of virology 74, 6614-6621.

Matsuyama, S., Ujike, M., Morikawa, S., Tashiro, M., and Taguchi, F. (2005). Protease-mediated enhancement of severe acute respiratory syndrome coronavirus infection. Proceedings of the National Academy of Sciences of the United States of America 102, 12543-12547.

Melikyan, G.B., Markosyan, R.M., Brener, S.A., Rozenberg, Y., and Cohen, F.S. (2000). Role of the cytoplasmic tail of ecotropic moloney murine leukemia virus Env protein in fusion pore formation. Journal of virology 74, 447-455.

Miller, D.G., Edwards, R.H., and Miller, A.D. (1994). Cloning of the cellular receptor for amphotropic murine retroviruses reveals homology to that for gibbon ape leukemia virus. Proceedings of the National Academy of Sciences of the United States of America 91, 78-82.

Mothes, W., Boerger, A.L., Narayan, S., Cunningham, J.M., and Young, J.A. (2000). Retroviral entry mediated by receptor priming and low pH triggering of an envelope glycoprotein. Cell 103, 679-689.

Munoz-Barroso, I., Salzwedel, K., Hunter, E., and Blumenthal, R. (1999). Role of the membrane-proximal domain in the initial stages of human immunodeficiency virus type 1 envelope glycoprotein-mediated membrane fusion. Journal of virology 73, 6089-6092.

Myszka, D.G., Sweet, R.W., Hensley, P., Brigham-Burke, M., Kwong, P.D., Hendrickson, W.A., Wyatt, R., Sodroski, J., and Doyle, M.L. (2000). Energetics of the HIV gp120-CD4 binding reaction. Proceedings of the National Academy of Sciences of the United States of America 97, 9026-9031.

Oakes, B., Tai, A.K., Cingoz, O., Henefield, M.H., Levine, S., Coffin, J.M., and Huber, B.T. (2010). Contamination of human DNA samples with mouse DNA can lead to false detection of XMRV-like sequences. Retrovirology 7, 109.

Ofek, G., Tang, M., Sambor, A., Katinger, H., Mascola, J.R., Wyatt, R., and Kwong, P.D. (2004). Structure and mechanistic analysis of the anti-human immunodeficiency virus type 1 antibody 2F5 in complex with its gp41 epitope. Journal of virology 78, 10724-10737.

Olsen, K.E., and Andersen, K.B. (1999). Palmitoylation of the intracytoplasmic R peptide of the transmembrane envelope protein in Moloney murine leukemia virus. Journal of virology 73, 8975-8981.

Opstelten, D.J., Wallin, M., and Garoff, H. (1998). Moloney murine leukemia virus envelope protein subunits, gp70 and Pr15E, form a stable disulfide-linked complex. Journal of virology 72, 6537-6545.

Ou, W., Lu, N., Yu, S.S., and Silver, J. (2006). Effect of epitope position on neutralization by anti-human immunodeficiency virus monoclonal antibody 2F5. Journal of virology 80, 2539-2547.

Pancera, M., Majeed, S., Ban, Y.E., Chen, L., Huang, C.C., Kong, L., Kwon, Y.D., Stuckey, J., Zhou, T., Robinson, J.E., Schief, W.R., Sodroski, J., Wyatt, R., and Kwong, P.D. (2010). Structure of HIV-1 gp120 with gp41-interactive region reveals layered envelope architecture and basis of conformational mobility.

Proceedings of the National Academy of Sciences of the United States of America 107, 1166-1171.

Pinter, A., Kopelman, R., Li, Z., Kayman, S.C., and Sanders, D.A. (1997). Localization of the labile disulfide bond between SU and TM of the murine leukemia virus envelope protein complex to a highly conserved CWLC motif in SU that resembles the active-site sequence of thiol-disulfide exchange enzymes. Journal of virology 71, 8073-8077.

Prizan-Ravid, A., Elis, E., Laham-Karam, N., Selig, S., Ehrlich, M., and Bacharach, E. (2010). The Gag cleavage product, p12, is a functional constituent of the murine leukemia virus pre-integration complex. PLoS pathogens 6, e1001183.

Ragheb, J.A., and Anderson, W.F. (1994). Uncoupled expression of Moloney murine leukemia virus envelope polypeptides SU and TM: a functional analysis of the role of TM domains in viral entry. Journal of virology 68, 3207-3219.

Rein, A., Mirro, J., Haynes, J.G., Ernst, S.M., and Nagashima, K. (1994). Function of the cytoplasmic domain of a retroviral transmembrane protein: p15E-p2E cleavage activates the membrane fusion capability of the murine leukemia virus Env protein. Journal of virology 68, 1773-1781.

Rice, N.R., Henderson, L.E., Sowder, R.C., Copeland, T.D., Oroszlan, S., and Edwards, J.F. (1990). Synthesis and processing of the transmembrane envelope protein of equine infectious anemia virus. Journal of virology 64, 3770-3778.

Robinson, M.J., Erlwein, O.W., Kaye, S., Weber, J., Cingoz, O., Patel, A., Walker, M.M., Kim, W.J., Uiprasertkul, M., Coffin, J.M., and McClure, M.O. (2010). Mouse DNA contamination in human tissue tested for XMRV. Retrovirology 7, 108.

Rodriguez, J.J., and Goff, S.P. (2010). Xenotropic murine leukemia virus-related virus establishes an efficient spreading infection and exhibits enhanced transcriptional activity in prostate carcinoma cells. Journal of virology 84, 2556-2562.

Rosen, C.A., Haseltine, W.A., Lenz, J., Ruprecht, R., and Cloyd, M.W. (1985). Tissue selectivity of murine leukemia virus infection is determined by long terminal repeat sequences. Journal of virology 55, 862-866.

Rosenberg, N., and Jolicoeur, P. (1997). Retroviral Pathogenesis.

Roux, K.H., and Taylor, K.A. (2007). AIDS virus envelope spike structure. Current opinion in structural biology 17, 244-252.

Sakuma, T., Tonne, J.M., Squillace, K.A., Ohmine, S., Thatava, T., Peng, K.W., Barry, M.A., and Ikeda, Y. (2011). Early Events in Retrovirus XMRV Infection of the Wild-Derived Mouse Mus pahari. Journal of virology 85, 1205-1213.

Salzwedel, K., West, J.T., and Hunter, E. (1999). A conserved tryptophan-rich motif in the membrane-proximal region of the human immunodeficiency virus type 1 gp41 ectodomain is important for Env-mediated fusion and virus infectivity. Journal of virology 73, 2469-2480.

Sanders, R.W., Schiffner, L., Master, A., Kajumo, F., Guo, Y., Dragic, T., Moore, J.P., and Binley, J.M. (2000). Variable-loop-deleted variants of the human immunodeficiency virus type 1 envelope glycoprotein can be stabilized by an intermolecular disulfide bond between the gp120 and gp41 subunits. Journal of virology 74, 5091-5100.

Sattentau, Q.J., and Moore, J.P. (1991). Conformational changes induced in the human immunodeficiency virus envelope glycoprotein by soluble CD4 binding. The Journal of experimental medicine 174, 407-415.

Schaal, H., Klein, M., Gehrmann, P., Adams, O., and Scheid, A. (1995). Requirement of N-terminal amino acid residues of gp41 for human immunodeficiency virus type 1-mediated cell fusion. Journal of virology 69, 3308-3314.

Schlaberg, R., Choe, D.J., Brown, K.R., Thaker, H.M., and Singh, I.R. (2009). XMRV is present in malignant prostatic epithelium and is associated with prostate cancer, especially high-grade tumors. Proceedings of the National Academy of Sciences of the United States of America 106, 16351-16356.

Senes, A., Engel, D.E., and DeGrado, W.F. (2004). Folding of helical membrane proteins: the role of polar, GxxxG-like and proline motifs. Current opinion in structural biology 14, 465-479.

Shang, L., and Hunter, E. (2010). Residues in the membrane-spanning domain core modulate conformation and fusogenicity of the HIV-1 envelope glycoprotein. Virology 404, 158-167.

Shang, L., Yue, L., and Hunter, E. (2008). Role of the membrane-spanning domain of human immunodeficiency virus type 1 envelope glycoprotein in cell-cell fusion and virus infection. Journal of virology 82, 5417-5428.

Shimizu, N., Tanaka, A., Oue, A., Mori, T., Ohtsuki, T., Apichartpiyakul, C., Uchiumi, H., Nojima, Y., and Hoshino, H. (2009). Broad usage spectrum of G protein-coupled receptors as coreceptors by primary isolates of HIV. AIDS (London, England) 23, 761-769.

Shimojima, M., Miyazawa, T., Ikeda, Y., McMonagle, E.L., Haining, H., Akashi, H., Takeuchi, Y., Hosie, M.J., and Willett, B.J. (2004). Use of CD134 as a primary receptor by the feline immunodeficiency virus. Science (New York, N.Y 303, 1192-1195.

Simmons, G., Gosalia, D.N., Rennekamp, A.J., Reeves, J.D., Diamond, S.L., and Bates, P. (2005). Inhibitors of cathepsin L prevent severe acute respiratory syndrome coronavirus entry. Proceedings of the National Academy of Sciences of the United States of America 102, 11876-11881.

Skehel, J.J., and Wiley, D.C. (2000). Receptor binding and membrane fusion in virus entry: the influenza hemagglutinin. Annual review of biochemistry 69, 531-569.

Smith, J.G., Mothes, W., Blacklow, S.C., and Cunningham, J.M. (2004). The mature avian leukosis virus subgroup A envelope glycoprotein is metastable, and refolding induced by the synergistic effects of receptor binding and low pH is coupled to infection. Journal of virology 78, 1403-1410.

Soll, S.J., Neil, S.J., and Bieniasz, P.D. (2010). Identification of a receptor for an extinct virus. Proceedings of the National Academy of Sciences of the United States of America 107, 19496-19501.

Song, L., Sun, Z.Y., Coleman, K.E., Zwick, M.B., Gach, J.S., Wang, J.H., Reinherz, E.L., Wagner, G., and Kim, M. (2009). Broadly neutralizing anti-HIV-1 antibodies disrupt a hinge-related function of gp41 at the membrane interface. Proceedings of the National Academy of Sciences of the United States of America 106, 9057-9062.

Spahn, C.M., and Penczek, P.A. (2009). Exploring conformational modes of macromolecular assemblies by multiparticle cryo-EM. Current opinion in structural biology 19, 623-631.

Stieler, K., Schulz, C., Lavanya, M., Aepfelbacher, M., Stocking, C., and Fischer, N. (2010). Host range and cellular tropism of the human exogenous gammaretrovirus XMRV. Virology 399, 23-30.

Suarez, T., Gallaher, W.R., Agirre, A., Goni, F.M., and Nieva, J.L. (2000a). Membrane interface-interacting sequences within the ectodomain of the human immunodeficiency virus type 1 envelope glycoprotein: putative role during viral fusion. Journal of virology 74, 8038-8047.

Suarez, T., Nir, S., Goni, F.M., Saez-Cirion, A., and Nieva, J.L. (2000b). The pre-transmembrane region of the human immunodeficiency virus type-1 glycoprotein: a novel fusogenic sequence. FEBS letters 477, 145-149.

Sullivan, N., Sun, Y., Sattentau, Q., Thali, M., Wu, D., Denisova, G., Gershoni, J., Robinson, J., Moore, J., and Sodroski, J. (1998). CD4-Induced conformational changes in the human immunodeficiency virus type 1 gp120 glycoprotein: consequences for virus entry and neutralization. Journal of virology 72, 4694-4703.

Sun, Z.Y., Oh, K.J., Kim, M., Yu, J., Brusic, V., Song, L., Qiao, Z., Wang, J.H., Wagner, G., and Reinherz, E.L. (2008). HIV-1 broadly neutralizing antibody extracts its epitope from a kinked gp41 ectodomain region on the viral membrane. Immunity 28, 52-63.

Swanstrom, R., and Wills, J.W. (1997). Synthesis, Assembly, and Processing of Viral Proteins.

Switzer, W.M., Jia, H., Hohn, O., Zheng, H., Tang, S., Shankar, A., Bannert, N., Simmons, G., Hendry, R.M., Falkenberg, V.R., Reeves, W.C., and Heneine, W. (2010). Absence of evidence of xenotropic murine leukemia virus-related virus infection in persons with chronic fatigue syndrome and healthy controls in the United States. Retrovirology 7, 57.

Tailor, C.S., Nouri, A., Lee, C.G., Kozak, C., and Kabat, D. (1999). Cloning and characterization of a cell surface receptor for xenotropic and polytropic murine leukemia viruses. Proceedings of the National Academy of Sciences of the United States of America 96, 927-932.

Taylor, G.M., and Sanders, D.A. (1999). The role of the membrane-spanning domain sequence in glycoprotein-mediated membrane fusion. Molecular biology of the cell 10, 2803-2815.

Taylor, G.M., and Sanders, D.A. (2003). Structural criteria for regulation of membrane fusion and virion incorporation by the murine leukemia virus TM cytoplasmic domain. Virology 312, 295-305.

Thali, M., Moore, J.P., Furman, C., Charles, M., Ho, D.D., Robinson, J., and Sodroski, J. (1993). Characterization of conserved human immunodeficiency virus type 1 gp120 neutralization epitopes exposed upon gp120-CD4 binding. Journal of virology 67, 3978-3988.

Urisman, A., Molinaro, R.J., Fischer, N., Plummer, S.J., Casey, G., Klein, E.A., Malathi, K., Magi-Galluzzi, C., Tubbs, R.R., Ganem, D., Silverman, R.H., and DeRisi, J.L. (2006). Identification of a novel Gammaretrovirus in prostate tumors of patients homozygous for R462Q RNASEL variant. PLoS pathogens 2, e25.

van Zeijl, M., Johann, S.V., Closs, E., Cunningham, J., Eddy, R., Shows, T.B., and O'Hara, B. (1994). A human amphotropic retrovirus receptor is a second member of the gibbon ape leukemia virus receptor family. Proceedings of the National Academy of Sciences of the United States of America 91, 1168-1172.

Vogt, V.M. (1997). Retroviral Virions and Genomes.

Waheed, A.A., Ablan, S.D., Roser, J.D., Sowder, R.C., Schaffner, C.P., Chertova, E., and Freed, E.O. (2007). HIV-1 escape from the entry-inhibiting effects of a

cholesterol-binding compound via cleavage of gp41 by the viral protease. Proceedings of the National Academy of Sciences of the United States of America 104, 8467-8471.

Waheed, A.A., Ablan, S.D., Sowder, R.C., Roser, J.D., Schaffner, C.P., Chertova, E., and Freed, E.O. (2010). Effect of mutations in the human immunodeficiency virus type 1 protease on cleavage of the gp41 cytoplasmic tail. Journal of virology 84, 3121-3126.

Wallin, M., Ekström, M., and Garoff, H. (2004). Isomerization of the intersubunit disulphide-bond in Env controls retrovirus fusion. The EMBO journal 23, 54-65.

Wallin, M., Ekström, M., and Garoff, H. (2005). The fusion-controlling disulfide bond isomerase in retrovirus Env is triggered by protein destabilization. Journal of virology 79, 1678-1685.

Wallin, M., Ekström, M., and Garoff, H. (2006). Receptor-triggered but alkylation-arrested env of murine leukemia virus reveals the transmembrane subunit in a prehairpin conformation. Journal of virology 80, 9921-9925.

Wang, H., Kavanaugh, M.P., and Kabat, D. (1994). A critical site in the cell surface receptor for ecotropic murine retroviruses required for amino acid transport but not for viral reception. Virology 202, 1058-1060.

Waning, D.L., Russell, C.J., Jardetzky, T.S., and Lamb, R.A. (2004). Activation of a paramyxovirus fusion protein is modulated by inside-out signaling from the cytoplasmic tail. Proceedings of the National Academy of Sciences of the United States of America 101, 9217-9222.

Weimin Wu, B., Cannon, P.M., Gordon, E.M., Hall, F.L., and Anderson, W.F. (1998). Characterization of the proline-rich region of murine leukemia virus envelope protein. Journal of virology 72, 5383-5391.

Weissenhorn, W., Dessen, A., Harrison, S.C., Skehel, J.J., and Wiley, D.C. (1997). Atomic structure of the ectodomain from HIV-1 gp41. Nature 387, 426-430.

White, T.A., Bartesaghi, A., Borgnia, M.J., Meyerson, J.R., de la Cruz, M.J., Bess, J.W., Nandwani, R., Hoxie, J.A., Lifson, J.D., Milne, J.L., and Subramaniam, S. (2010). Molecular architectures of trimeric SIV and HIV-1 envelope glycoproteins on intact viruses: strain-dependent variation in quaternary structure. PLoS pathogens 6, e1001249.

Wu, S.R., Sjoberg, M., Wallin, M., Lindqvist, B., Ekstrom, M., Hebert, H., Koeck, P.J., and Garoff, H. (2008). Turning of the receptor-binding domains opens up the murine leukaemia virus Env for membrane fusion. The EMBO journal 27, 2799-2808.

Wyatt, R., Moore, J., Accola, M., Desjardin, E., Robinson, J., and Sodroski, J. (1995). Involvement of the V1/V2 variable loop structure in the exposure of human immunodeficiency virus type 1 gp120 epitopes induced by receptor binding. Journal of virology 69, 5723-5733.

Wyss, S., Dimitrov, A.S., Baribaud, F., Edwards, T.G., Blumenthal, R., and Hoxie, J.A. (2005). Regulation of human immunodeficiency virus type 1 envelope glycoprotein fusion by a membrane-interactive domain in the gp41 cytoplasmic tail. Journal of virology 79, 12231-12241.

Yang, C., and Compans, R.W. (1997). Analysis of the murine leukemia virus R peptide: delineation of the molecular determinants which are important for its fusion inhibition activity. Journal of virology 71, 8490-8496.

Yang, Y.L., Guo, L., Xu, S., Holland, C.A., Kitamura, T., Hunter, K., and Cunningham, J.M. (1999). Receptors for polytropic and xenotropic mouse leukaemia viruses encoded by a single gene at Rmc1. Nature genetics 21, 216-219.

Zanetti, G., Briggs, J.A., Grunewald, K., Sattentau, Q.J., and Fuller, S.D. (2006). Cryo-electron tomographic structure of an immunodeficiency virus envelope complex in situ. PLoS pathogens 2, e83.

Zavorotinskaya, T., and Albritton, L.M. (1999). A hydrophobic patch in ecotropic murine leukemia virus envelope protein is the putative binding site for a critical tyrosine residue on the cellular receptor. Journal of virology 73, 10164-10172.

Zhou, T., Xu, L., Dey, B., Hessell, A.J., Van Ryk, D., Xiang, S.H., Yang, X., Zhang, M.Y., Zwick, M.B., Arthos, J., Burton, D.R., Dimitrov, D.S., Sodroski, J., Wyatt, R., Nabel, G.J., and Kwong, P.D. (2007). Structural definition of a conserved neutralization epitope on HIV-1 gp120. Nature 445, 732-737.

Zhou, T., Georgiev, I., Wu, X., Yang, Z.Y., Dai, K., Finzi, A., Kwon, Y.D., Scheid, J.F., Shi, W., Xu, L., Yang, Y., Zhu, J., Nussenzweig, M.C., Sodroski, J., Shapiro, L., Nabel, G.J., Mascola, J.R., and Kwong, P.D. (2010). Structural basis for broad and potent neutralization of HIV-1 by antibody VRC01. Science (New York, N.Y 329, 811-817.

Zhu, N.L., Cannon, P.M., Chen, D., and Anderson, W.F. (1998). Mutational analysis of the fusion peptide of Moloney murine leukemia virus transmembrane protein p15E. Journal of virology 72, 1632-1639.

Zhu, P., Liu, J., Bess, J., Jr., Chertova, E., Lifson, J.D., Grise, H., Ofek, G.A., Taylor, K.A., and Roux, K.H. (2006). Distribution and three-dimensional structure of AIDS virus envelope spikes. Nature 441, 847-852.